DEVELOPMENT OF Q-SWITCHED AND MODELOCKED ERBIUM-DOPED FIBER LASERS (EDFL) BASED ON GOLD NANOPARTICLES (GNP) AS SATURABLE ABSORBER

NURSYAZANA BINTI ZAINAL ABIDIN

FACULTY OF ENGINEERING
UNIVERSITY OF MALAYA
KUALA LUMPUR

2019

DEVELOPMENT OF Q-SWITCHED AND MODELOCKED ERBIUM-DOPED FIBER LASERS (EDFL) BASED ON GOLD NANOPARTICLES (GNP) AS SATURABLE ABSORBER

NURSYAZANA BINTI ZAINAL ABIDIN

SUBMITTED TO THE FACULTY OF ENGINEERING UNIVERSITY OF MALAYA, IN PARTIAL FULFILMENT OF THE REQUIREMENTS FOR THE DEGREE OF MASTER OF ENGINEERING (TELECOMMUNICATIONS)

FACULTY OF ENGINEERING

UNIVERSITY OF MALAYA

KUALA LUMPUR

2019

UNIVERSITY OF MALAYA

ORIGINAL LITERARY WORK DECLARATION

Name of Candidate: NURSYAZANA BINTI ZAINAL ABIDIN

Matric No: KQH160004

Name of Degree: MASTER OF ENGINEERING (TELECOMMUNICATIONS)

Title of Project Paper/Research Report/Dissertation/Thesis ("this Work"):

DEVELOPMENT OF Q-SWITCHED AND MODELOCKED ERBIUM-DOPED FIBER LASERS (EDFL) BASED ON GOLD NANOPARTICLES (GNP) AS SATURABLE ABSORBER

Field of Study: ENGINEERING SCIENCES (FIBER LASER)

I do solemnly and sincerely declare that:

(1) I am the sole author/writer of this Work;
(2) This Work is original;
(3) Any use of any work in which copyright exists was done by way of fair dealing and for permitted purposes and any excerpt or extract from, or reference to or reproduction of any copyright work has been disclosed expressly and sufficiently and the title of the Work and its authorship have been acknowledged in this Work;
(4) I do not have any actual knowledge nor do I ought reasonably to know that the making of this work constitutes an infringement of any copyright work;
(5) I hereby assign all and every rights in the copyright to this Work to the University of Malaya ("UM"), who henceforth shall be owner of the copyright in this Work and that any reproduction or use in any form or by any means whatsoever is prohibited without the written consent of UM having been first had and obtained;
(6) I am fully aware that if in the course of making this Work I have infringed any copyright whether intentionally or otherwise, I may be subject to legal action or any other action as may be determined by UM.

Candidate's Signature Date:

Subscribed and solemnly declared before,

Witness's Signature Date:

Name:

Designation:

ABSTRACT

In this experiment, we experimentally demonstrate a Q-switched and mode-locked Erbium-doped fiber lasers (EDFLs) using gold nanoparticle (GNPs) which is embedded into a polyvinyl alcohol (PVA) film as a passive saturable absorber (SA). The film is sandwiched between two ferrules via a fiber connector to form a fiber-compatible SA and integrated into the laser cavity for Q-switching and mode locking pulse generation in a 14.8m cavity length. The laser produces a successful stable q-switched pulse train operating at 1564.2nm within the incident pump power ranging from 63.4mW to 92.3mW. The achieved repetition rate ranges from 49.4kHz to 56.8kHz and the pulse width can be as narrow as 4.16µs. A 200-m long standard single mode fiber (SMF) is added to the cavity to achieve stable mode-lock nanosecond pulses at 1567nm with spectral width of 1.1nm. Furthermore, a pulse duration of 450ns and a repetition rate of 970kHz is achieved. The average output power is 2.48mW, which corresponds to a single pulse energy of 25.5nJ at pump power of 187mW.

ABSTRAK

Bagi penyelidikan ini, kami membuat eksperimen mendemostrasikan suis-Q dan Penyelakan Mod laser gentian terdop erbium (EDFL) menggunakan zarahnano emas (GNPs) dimana ia telah diterapkan ke dalam alkohol polivinil (PVA) sebagai penyerap tetepu (SA). Terapan ini dimasukkan antara dua kepala gentian untuk membentuk kesesuaian-gentian SA dan disepadukan ke dalam litar laser untuk menjana pulsa bagi suis-Q dan Penyelakan Mod di dalam 14.8m litar. Laser ini telah menjana pulsa suis-Q yang stabil yang beroperasi pada 1564.2nm dalam lingkungan di antara 63.4mW hingga 92.3mW kuasa pam. Ia juga mencapai kadar ulangan dari 49.4kHz hingga 56.8kHz dan lebar pulsa yang dicapai pula adalah sekecil 4.16µs. Seterusnya, 200m panjang gentian mod tunggal telah ditambah ke dalam litar untuk mencapai pulsa nanosaat Penyelakan Mod yang stabil pada 1567nm dengan kelebaran spectrum 1.1nm. Laser ini turut mencapai durasi pulsa 450ns dan kadar ulangannya adalah 970kHz. Manakala, purata kuasa output ialah 2.48mW dimana ia sepan dengan kuasa pulsa tunggal 25.5nJ pada 187mW kuasa pam.

ACKNOWLEDGEMENTS

First and foremost, I would like to express my utmost gratitude towards Allah SWT for providing me this opportunity and granting me the capability to increase my knowledge and to successfully accomplish this thesis. I would also like to thank my respected supervisor, PROF. DR. SULAIMAN WADI HARUN, for without your trust, endless patience, thoughtful guidance and valuable advice, I would not be able to develop my research skills and complete this project successfully. Thank you for seeing the potential in me. To FARHANAH and FARINA, I greatly appreciate your friendly assistance regarding my project. Truly, your contributions have helped me enormously. A massive thanks to SYAZWANI IZRAH and AERIYN DWIERNI, you have provided a helping hand to me in many different ways. To my close friends, thank you for your useful suggestions and words of encouragement. Finally, I warmly thank and appreciate my parents, ZAINAL ABIDIN MOHD RAWI and SUMIAH YAAKUB, my brothers, AMIN, AZIM, AIMAN, and sister-in-law, AIN, for your endless prayers, motivation and material support. Your infinite encouragement and support have given me the strength and motivation to carry on. A special thanks to my lovely nephew, UMAR CALIPH, whose adorable antics have cheered me up in my toughest times. Thank you.

TABLE OF CONTENTS

LIST OF FIGURES

LIST OF SYMBOLS AND ABBREVIATIONS

LASIK	:	Laser-Assisted In-situ Keratomileusis
WDM	:	Wavelength Division Multiplexing
CW	:	Continuous Wave
EDF	:	Erbium-Doped Fiber
EDFA	:	Erbium-Doped Fiber Amplifier
EDFL	:	Erbium-Doped Fiber Laser
Er	:	Erbium
Yt	:	Ytterbium
Nd	:	Neodymium
Tm	:	Thulium
Pr	:	Praseodymium
Ho	:	Holmium
Dy	:	Dysprosium
FWHM	:	Full Width Half Maximum
OSA	:	Optical Spectrum Analyzer
OSC	:	Oscilloscope
SA	:	Saturable Absorber
PVA	:	Polyvinyl Alcohol
RF	:	Radio Frequency
CNT	:	Carbon Nanotube
SESAM	:	Semiconductor Saturable Absorber Mirrors
SNR	:	Signal to Noise Ratio
TI	:	Topology Insulators
GNP	:	Gold Nanoparticle
MCVD	:	Modified Chemical Vapour Deposition
Xe	:	Xenon
ASE	:	Amplified Spontaneous Light
MQW	:	Multiple Quantum Well

PSSS	:	Polysodium-4-styrenesulforate
$HAuCL_4$	:	Gold (III) chloride trihydrate
$Na3C6H_5O_7$	:	Trisodium Citrate
$NaBH_4$	:	Sodium Borohydrate
NP	:	Nanoparticle
Au	:	Gold
TEM	:	Transmission Electron Microscopy
SEM	:	Scanning Electron Microscopy
SMF	:	Single-Mode Fiber
GVD	:	Group Velocity Dispersion
CuNW	:	Copper Nano Wire
SPR	:	Surface Plasmon Resonance
NPR	:	Nonlinear Polarization Rotation
2D	:	Two-Dimension
TMP	:	Transition Metal Dichalcoganides

CHAPTER 1:

INTRODUCTION

1.1 Introduction

Fiber lasers have been progressively developing in various areas of scientific and technological advances since its initial development in the early 1960s. The qualities and features of fiber lasers have been made to good use and applied in telecommunications, medical diagnosis and treatment, material processing, environmental monitoring, and military defense. The continuous study on fiber laser knowledge and improvements on its applications have made our everyday lives much easier.

Fiber laser-based machines with high intensity and pulse energy have been widely used in micromachining, cutting and drilling in the manufacturing industry. Fiber lasers which are based on optical fibers can be designed to be highly precise and accurate while having low scattering loss and undesired absorptions. Other than that, fiber lasers are also actively used in the medical industry in the areas of therapy, diagnostics, cosmetics, research and in various types of surgery. The most commonly known medical treatment using laser is in eye surgery called LASIK, a short for Laser-Assisted in-situ Keratomileusis. It is a medical procedure to permanently change the shape of the cornea by removing a thin layer of corneal tissue using laser in order to improve vision thus reducing the patient's need to wear prescription glasses or contact lenses. This procedure is possible due to the flexibility and the small size of the fiber laser (Gursel, 2018; Shi, Schulzgen, Amezcua, Zhu, & Alam, 2017).

In the telecommunication industry, traditional diode laser transmitters have been replaced with fiber laser system developed as a telecom transmitter which has lower cost and will boost performance in the wavelength division multiplexing (WDM) networks. Due to the cylindrical geometry and compact and light characteristics of fiber laser, the system setup location can be flexibly positioned, thus reducing size and saving cost.

Furthermore, in order to meet the growing user demands of a higher speed data rate transmission and far-field network coverage, transmission fiber which is efficiently coupled with laser light produces long-distance propagation have been widely applied in optical transmission technology. Fiber laser's ability to tune wavelengths is also a major attention in the telecommunication industry.

Fundamentally, fiber laser is defined as a type of solid-state laser with doped fiber as the active gain medium. An active optical fiber is produced by coupling doped fiber amplifier with its core which is doped in one of the rare-earth materials or their mixture, thus providing light amplifications without lasing. This practically means that a fiber amplifier which usually functions to boost optical signals can be converted into a fiber laser by putting it inside the cavity made to attain response. Fiber laser offers output wavelength which can be varied, where the lasing wavelength is determined by the rare-earth dopant which is merged in the core of the fiber. Absorption of photons at the pump beam wavelength happens and stimulated emission produces a lasing output having the wavelength of the dopant in the fiber (Fermann & Hartl, 2013; Zervas & Codemard, 2014). In simpler words, rare-earth metal ions absorb pump beam at a shorter wavelength than the laser wavelength which permits amplified light with stimulated emission. These kinds of doped fibers are named active fibers with highly efficient gain media due to captivity of strong beam.

An important characteristic of rare-earth ion lasers is that the output spectral property is greatly affected by the molecular environment that the rare earth ions are in. this means that by tuning the composition of the host material, the lasing spectrum can be differed. The rare elements that are typically used as dopants are erbium (Er), ytterbium (Yb), neodymium (Nd), thulium (Tm), praseodymium (Pr), holmium (Ho), or dysprosium (Dy). However, Erbium has been actively used as a dopant since the element has high useful energy levels which results in lower cost for diode laser pump but still provides a high energy output.

Lasers can be utilized in different modes of operation namely continuous wave (CW), quasi CW, Q-switch, gain-switch, mode-lock and Q-switched mode-lock. The most commonly used modes are Q-switch and mode lock modes. Q-switch mode produces pulses going from micro to nanoseconds. It is a means to attain short and powerful pulses of laser ranging from a few megawatts to a few tens of megawatts. The term 'Q-switching' refers to a sudden change of the laser resonator *Q* factor from a low to a high value. On the other hand, mode-locking is a technique that generates super short optical pulses in the range of femtoseconds. In order to obtain this pulse, the phases of oscillating axial laser modes which have a faint difference in frequencies are locked together. Constructive interference between these modes eventually results in the laser beam to be generated as a train of pulses (Ahmed, 2015; Haus, 2000; Villegas et al., 2011).

Q-switch and mode-lock modes have active and passive methods of pulse generation. Active Q-switching includes the presence of an active control element, normally an electro-optic or an acousto-optic modulator. Active mode-locking is produced by relying on an external element positioned into the laser cavity, for example, a fast-modulating crystal, which results in the self-modulation of light. Passive method for both Q-switch and mode-lock is obtained using some kind of saturable absorber (SA).

A saturable absorber refers to an optical component which its optical loss is reduced at high light intensities. In previous researches, different types of SAs have been used and proposed such as the semiconductor saturable absorber mirror (SESAM) (Keller et al., 1996), quantum dots (Lee, Chen, Huang, Chen, & Jiang, 2016), gallium arsenide, graphene layers (Ahmed, 2015; Bao et al., 2009; Chernysheva et al., 2016; Sun et al., 2009), Cr^{4+}:YAG, and carbon nanotubes (CNTs) (Ahmed, 2015; Chernysheva et al., 2016; Sun et al., 2009) for the applications of passive Q-switch and mode-lock.

1.2 Objectives

The research aims at the development of Q-switched and mode-locked pulses by using gold nanoparticles (GNPs) as saturable absorbers. This objectives of this work are precisely outlined as follows:

- To experimentally generate a passively Q-switched fiber laser using Erbium-doped fiber as the gain medium and gold nanoparticles as saturable absorber
- To experimentally demonstrate mode-locked fiber laser using gold nanoparticles based saturable absorber.

1.3 Outline of This Project

This thesis holistically reports the fiber laser introduction, the working principle, experimental methods, experimental results and discussion along with data analysis on the generation of Q-switched and mode-locked Erbium-doped fiber laser (EDFL) based on gold nanoparticle (GNP) as the saturable absorber. This report is organized into five chapters. Chapter 1 briefly introduces fiber laser and its characteristics and applications in the industry. Other than that, the objectives and overview of this research is outlined. Chapter 2 gives the detailed theoretical background and fundamental knowledge along with the mentions from the previous researches. Chapter 3 introduces the research methodology on how the experiment is done. The configurations of both Q-switched and mode-locked lasers will also be described in this chapter. The materials used and also devices used to measure the parameters involved are shown. Chapter 4 describes and discusses the result of the generation of Q-switch and mode-locked pulse in similar EDFL setup using GNP as the saturable absorber. This chapter analyses the performances in terms of its pump power, repetition rate, pulse width, and output power.. Finally, Chapter 5 concludes and compares the results of both procedures and proposes the future direction of this work.

CHAPTER 2:

LITERATURE REVIEW

2.1 History of fiber laser

Fiber laser have turned into a significant device in building innovation, fundamental science and in expansive scope of useful applications. The first fiber laser development is credited to Snitzer and his colleagues, in the early 1960s, when they published the findings for the amplifications of a multicomponent glass fiber laser (C. J. Koester & Snitzer, 1964; Snitzer, 1964). Not long after, Tippet and his team have considered the possibility of optical information data to be processed using fiber lasers in his research (Tippett, Borkowitz, Clapp, Koester, & Vanderburgh Jr, 1965). Other than that, Koester have observed an oscillation and amplification between a passive core and a laser cladding (C. Koester, 1966).

Though there are many published findings and developments in the early stages of the subject, not many publications are found from the late 1970s to the early 1980s (Urquhart, 1988). However, in 1985, a research originating from the Southampton University Electrical Engineering and Physics Department have rekindled the interest of many in fiber lasers when they demonstrated the production of fibers containing rare-earth ions through the process of extended modified chemical vapour deposition (MCVD) method (Poole, Payne, & Fermann, 1985).

The fiber laser discipline continued to develop in the 1990s, where many new experiments and novel ideas are in abundance. The advancement is greater when optical fibers are doped with rare-earth elements such as Erbium, Ytterbium, Holmium, and Thulium to be fabricated as amplifiers and lasers (Agrawal, 2001) along with the discovery of new modes of laser operation that have enhanced its previous constraints in terms of pulse energy and duration which eventually results in the creation of light pulses with very short time span (Csele, 2011; Gursel, 2018).

2.2 Fiber laser operation

Fundamentally, a fiber laser is a type of solid-state laser where the active medium being utilized is an optical fiber that has been doped with rare-earth ions (Digonnet, 2001; C. J. Koester & Snitzer, 1964). A basic structure of a longitudinally pumped fiber laser is visualized in Figure 2.1 below. It shows an optical fiber, for which the core that has been doped with rare-earth elements is clamped between two mirrors.

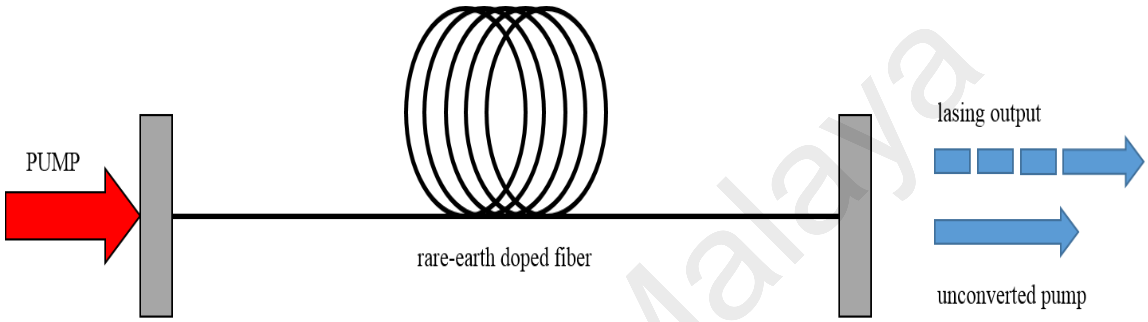

Figure 2.1: Schematic diagram of a fiber laser

It works such that light is propelled through the mirror on the left from a 'pumping laser' and the output beam from the fiber laser is coupled through the mirror on the right Here, absorption of photons at the wavelength of the pump beam happens and causes an inverted population and a right amount of stimulated emission thus amplifies at the wavelength characteristic of which the fiber is doped in (Urquhart, 1988). The reflection of light in the cavity causes the group of photons to stimulate the atoms to discharge energy at different wavelengths.

An atom has two energy states, which are ground and exited states. An atom stays at the ground state when its energy is at the lowest and most stable. When an electron absorbs energy, it is excited and its energy level is elevated. Over time, the electron losses energy and drops back to lower energy level. Then, photons of different wavelengths releases energy and this prompts other electrons to give out more in-phase photons (Addanki, Amiri, & Yupapin, 2018; Melton, Riahinasab, Keshavarz, Stokes, & Hirst, 2018). Figure 2.2 shows a simple energy level diagram.

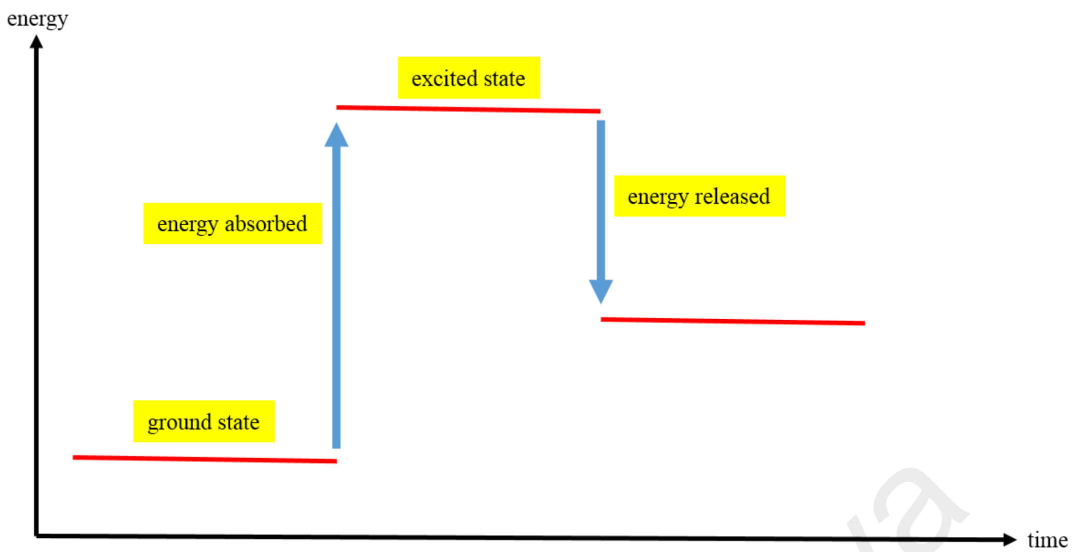

Figure 2.2: Energy level diagram

Following this statement, it can be said that a fiber laser is in fact a wavelength converter and a waveguiding structure, where the output wavelength variation depends on the dopant of the fiber. Not only do fiber lasers offer a wide range of output wavelengths, they are also robust in design. These benefits have many great practical uses in many applications in the industry, namely telecommunications, medicine, manufacturing and many more (Ahmed, 2015; Mur, 2011; Urquhart, 1988).

2.3 Erbium-doped fiber laser

Glass fiber lasers are often doped with rare-earth metal ions. Optical fibers made from plastic are not always utilized because plastic fibers are difficult to dope, usually have more than one modes, has high absorption rate and is quite delicate when it comes to light with high intensities. Rare-earth metal ions absorb pump light at a shorter wavelength than the laser wavelength (Mur, 2011). The rare earth elements, or scientifically known as the lanthanides, are a series of fifteen metallic chemical elements with the atomic numbers starting from 57 up to 71. Each rare-earth ions have similar outer electronic structure of $5s^2 5p^6 6s^2$. As shown in the figure below, the 5s and 5p electrons is replaced with the element Xenon, Xe where their optical absorption and emission depends on the electrons at the inner 4*f* shell (France, 1988).

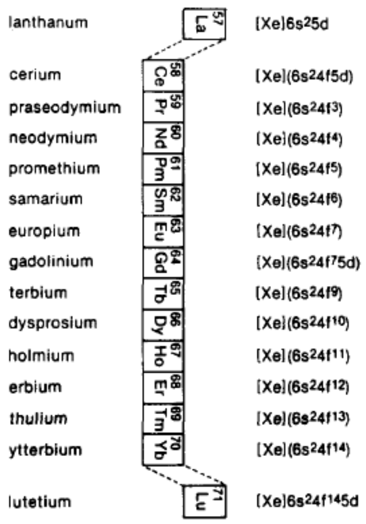

Figure 2.3: The rare earth elements displaying atomic numbers and electronic configuration (France, 1988)

Development of rare-earth doped fiber laser started with the constant utilization of the element Neodymium doped in glass fiber because it's efficient Nd^{3+} ions as a laser. At the same time, Erbium-doped glass laser has garnered interest due to its safe optical features. Other than that, Erbium-doped fiber laser has a small range of transmission loss in fiber optic communications. Early development of erbium ions doped in glass fibers have been reported in late 1980s where reports show that Er^{3+} have a wavelength of 1.55µm, which is much needed in optical communications (Astakhov, Butusov, Galkin, Ermakova, & Fedorov, 1987; Desurvire & Simpson, 1989; Mears, Reekie, Poole, & Payne, 1986). A similar study also suggests that particularly Er^{3+} ions have a potential use due to its range of emission wavelength between 1500nm to 1600nm which is often utilized in optical fiber communications (Ainslie, Craig, & Davey, 1988).

Figure below shows the Stark level manifolds of Er^{3+} ions in an erbium-doped fiber in silicate glass. Stark splitting, which is the outcome of the Stark effect, is used to determine the form of the energy levels and spectral line. The Stark effect happens when the spectral lines are shifted and split because of the static electric field which is applied externally. The splitting of the energy level of rare-earth ions depends on the host material, which in this example is Er^{3+} in a glass host. The Stark levels of each energy is partly determined by the number of electrons present in the particular ion and also the quantum value of the angular momentum. In this example, the Stark levels are labeled at the left side of the diagram while the numbers at the right indicates the wavelength of the ground state absorption transition measured in nanometers (Digonnet, 2001; Steinkemper, Fischer, Hermle, & Goldschmidt, 2013). In lasers, the behavior of erbium ions can be seen as a quasi-three-level system(Yao, Thévenaz, & Brès, 2017).

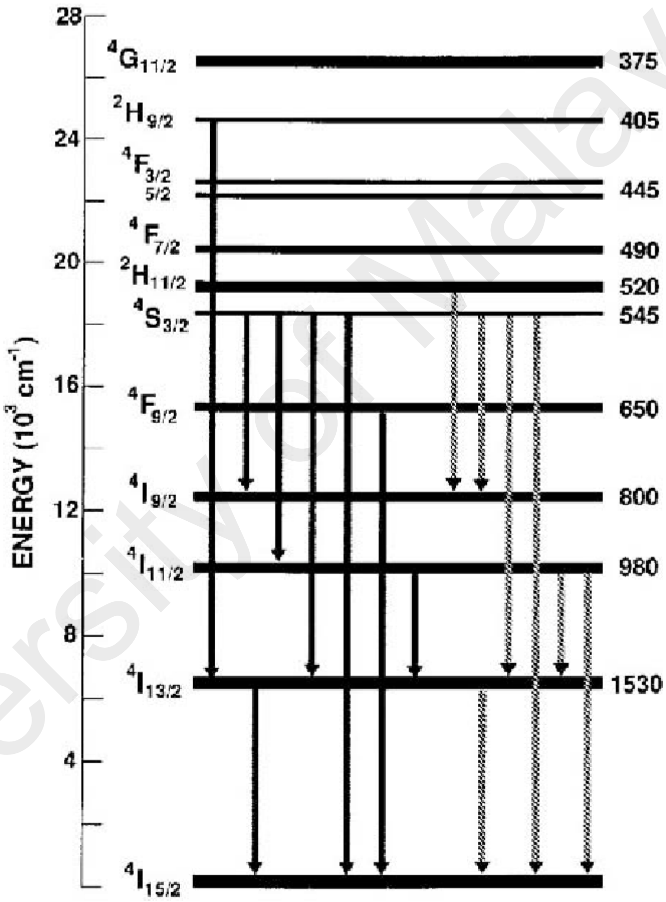

Figure 2.4: Energy level diagram of an EDF

From the diagram above, it shows that, from the ground state $^4I_{15/2}$, the erbium absorption transition to levels $^4I_{9/2}$, $^4I_{11/2}$, and $^4I_{13/2}$ are at bands of 800nm, 980nm, and 1550nm respectively. While the fluorescence of erbium from $^4I_{13/2}$ to $^4I_{15/2}$ is at 1550nm range. This means that for erbium, lasing is possible within the 1550nm range while pumping is available at 880nm and 980nm absorption bands. It is also observed that there is an overlap of the absorption band and the fluorescence band at 1550nm. When the EDF is pumped with 980 pump, photon absorption of Er^{3+} ions increases it to level $^4I_{11/2}$ before releasing energy towards level $^4I_{13/2}$. A population inversion between $^4I_{11/2}$ and the ground state happens through constant pumping, which then outputs spontaneous and stimulated photons in 1550nm region. In the laser cavity, the amplified spontaneous light (ASE) oscillates and eventually generates an output laser.

2.4 Q-switching

Q-switch is a technique where the laser produces high active short pulses at many roundtrips in a duration through modulation of the losses in the cavity Q of the laser resonator (Degnan, 1989; Haus, 2000). It works such that when an amount of energy is pumped into the resonator cavity, gain value in the cavity increases exponentially until it reaches a maximum level and will result in saturation eventually. At this point, the laser resonator Q factor toggles from high level to low level suddenly and produces short and intense pulses of light (Lü, Han, Liu, Chen, & Ren, 2014). The typical pulse width range obtained through q-switching is from picoseconds to nanoseconds (Dong & Samson, 2016), while the pulse repetition rate is between 1 up to a 100 kHz (Tiu, 2015). A q-switch configuration can be seen in Figure 2.5 below.

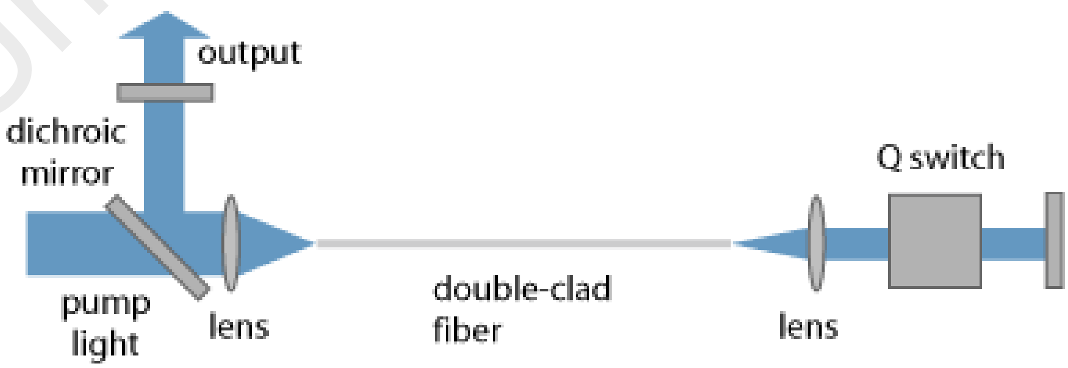

Figure 2.5: An Active Q-switch setup

Q-switching operation can be achieved through two techniques which are active and passive techniques. In active q-switching, the modulation of the losses is controlled by an active element externally generated electrically such as an electro-optic (Jabczyński, Zendzian, & Kwiatkowski, 2006) or an acousto-optic modulator (Li, Zhu, & Zhang, 2015). Fundamentally, the stored energy in the cavity is determined by the pulse energy and pulse duration. Subsequently, the pump power controls the pulse repetition rate, pulse energy, and also the pulse width. However, this method requires expensive bulky devices with drawbacks such as high driving voltage, unstable and complex (Carruthers, Duling, & Dennis, 1994).

On the other hand, the laser resonator can also be switched passively by using a saturable absorber which is much easier and reduces the complexity and size of the cavity design by eliminating the external modulator device. The generation of pulse happens when the energy kept in the gain medium has reached a constant value which indicates the saturation level. The saturable absorbers, of if its recovery time is larger than the pulse duration, is able to eliminate unnecessary energy loss. Some examples of saturable absorbers include semiconductor saturable absorber mirrors (SESAMs), graphene (Popa et al., 2011), quantum dots (Lee et al., 2016) and carbon nanotubes (Chernysheva et al., 2016).

2.5 Mode-locking

The term mode-locking refers to the process of locking together multiple oscillating longitudinal axial laser modes in a laser cavity where each modes have slightly different frequencies. The generation of the resulting ultra short optical pulses in the range of femtoseconds is through the constructive interference of these different modes which are locked with one another. The mutual interference produces a lasing output in the form of a periodic train of pulses as seen in Figure 2.6. As the number of modes locked together increases, the output pulse becomes narrower (Haus, 2000; Urquhart, 1988). Similar to Q-switching, mode-locking technique also has active and passive methods of operation.

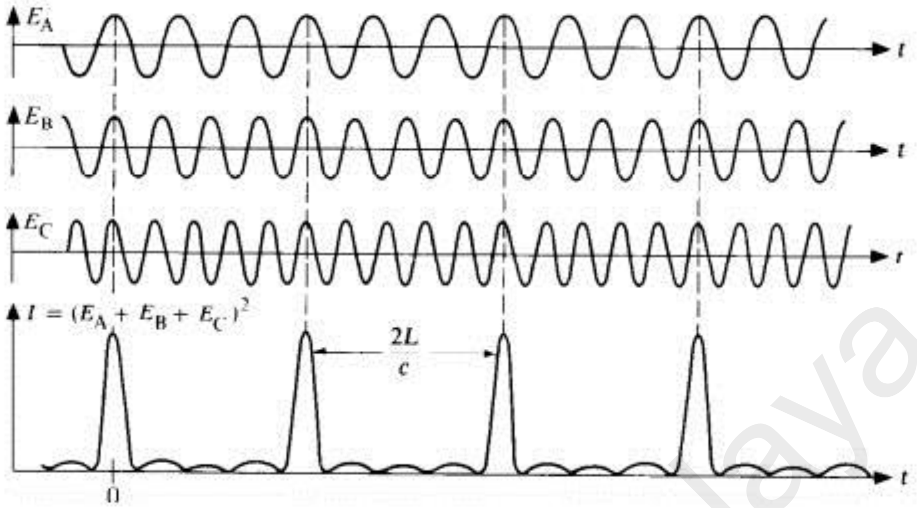

Figure 2.6: Formation of train of pulses through mode-locking technique

Active methods refers to the self-modulation of light by utilizing external signals which have some elements being placed inside the laser cavity. It is achieved by implementing in the cavity an optical modulation device such as an acousto-optic (Villegas et al., 2011) and an electro-optic modulator (Malmström, Margulis, Tarasenko, Pasiskevicius, & Laurell, 2012). Active techniques are however very complex and increases the size of the cavity due to the bulky nature of the modulator.

Passive methods, on the other hand, results in a self-produced variation in the light cavity by due to the change in some of the elements in the cavity (Hudson, 2009). It is achieved by replacing the modulator with a saturable absorber such as semiconductor saturable absorber mirrors (SESAMs), graphene oxide layers (H.-R. Chen, Tsai, Cheng, Lin, & Hsieh, 2014), and carbon nanotubes (CNTs) (Ahmed, 2015). Although SESAMs are widely used in pulse generation through mode-locking, the process to fabricate it is quite difficult as it has certain requirements that need to be fulfilled in order to lessen the time of recovery (Keller & Paschotta, 2002). Alternatively, CNT and graphene oxide layers as saturable absorbers involves much simpler fabrication process with benefits of shorter recovery time and is able to operate in a wider bandwidth (Sobon, Sotor, & Abramski, 2012; Sun et al., 2009).

2.6 Saturable Absorber

A saturable absorber is an optical element or material, of which its optical loss is reduced at high optical intensities. The optical loss is possible in a gain medium with absorbing dopant ions, when a strong optical intensity leads to the depletion of the ground state of this ions. It has been described as the main component for passive method for short pulse generation in both Q-switch and mode-lock laser operations. The saturable absorption process is described with resemblance to the two energy level system consisting energy levels for valence band, E_v and conduction band, E_c.

The original report of mode-locking with SA was using rhodamine-based organic dye (Mocker & Collins, 1965). The team have managed to successfully generate a pulse width in the range of 10 ns. De Maria and her team then accomplished pulse widths on the order of picoseconds (DeMaria, Stetser, & Heynau, 1966). In mid 1980s, femtosecond pulses as short as 27 fs right from a laser oscillator has been reported (Valdmanis & Fork, 1986). By the early1990s, progresses in semiconductor growth processes and bandgap engineering brings to the birth of semiconductor saturable absorber mirrors (SESAMs) (Keller et al., 1996).

SESAM, an advanced technology in semiconductor, is a mirror structure with an built-in saturable absorber. It is predominantly used for passive Q-switching or mode-locking (Shen, 2012). This technology involves the application of multiple quantum well (MQW) structures or quantum dot structures that produces controlled bandgap with high precision, and also thermalization procedures in the range of 10 to 100 femtoseconds, and can be robustly designed and made to have a long lifespan for the device. Fabrication of SESAMs involves the semiconductor material used and the device geometry, in order to be operable in the near infrared but up to the 1550nm C-band for fiber optic use.

Individual SESAMs can also be tunable over the range of 100s nm. However, SESAMs are complex, high fabrication cost, can only operate in a small range of wavelength, require expensive clean room equipment and have low damage threshold and long recovery time (Ahmed, 2015).

As mentioned above, SESAMs, graphene oxide layers, CNTs are often used saturable absorbers for passive q-switched and mode-locked fiber lasers. Despite many methods and new materials are explored in developing the SA for Q-switching pulse generation, metal nanoparticles-based SA especially transition metal elements are rarely being investigated. These elements pick up a great interest amongst scientific researchers as they hold a unique optical property such as ultrafast response time, broad saturable absorption band and large third-order nonlinearity (Sobon, 2015).

2.7 Optical measurements of fiber laser

The experiment setup involves many equipments in order to measure the parameters of fiber laser. An optical spectrum analyzer is used to analyze the wavelength spectrum. The repetition rate and pulse width are measured using the oscilloscope connected to the photo-detector. The autocorrelator is used to measure the full width at half-maximum (FWHM) while the powermeter is used to measure the input and output power. The pulse energy and peak power formulae are further explained below.

Pulse energy, E_p is the total optical energy content of the pulse. The pulse energy is calculated by dividing the average output power P_o, which is measured using the powermeter) by the repetition rate R_R (measured with oscilloscope).

$$Ep \approx \frac{P_o}{R_R}$$

Typical pulse energy for Q-switched laser ranges from microjoules to millijoules. While mode-locked laser achieves much lower pulse energy ranging from nanojoules to picojoules, due to mode-lock having high pulse repetition rate. The pulse energy together with the pulse duration are used to calculate the peak power of the laser pulse.

Peak power, P_p is the maximum optical power of the pulse. Due to the short pulse duration, which is possible for optical pulse, the peak power can become very high even for moderately energetic pulse. The peak power can be calculated from the FWHM pulse duration, τ_p, which is measured by an optical autocorrelator and the pulse energy, $E_{p.}$ the conversion depends on the pulse shape, for example a soliton pulse is given by

$$P_P \approx 0.95 \frac{E_p}{\tau_p}$$

Repetition rate represent pulses that are generated by the laser per second. Usually, Q-switched laser will produce 1Hz to 100kHz repetition rate. While repetition rate with range of 50MHz to 1GHz are usually produced by Mode locked laser. Both the repetition rate mentioned above will sometimes be different depend on the pump power that are pump into the cavity.

Another name for Pulse Width or pulse duration is full width at half maximum (FWHM) amplitude. This amplitude is the amplitude of the pulse laser in the graph. The graph that are referred is the optical power versus time graph. Q-switching and mode locking produce different pulse duration. Both Q-switching and Mode locking usually will produce nanosecond range and picosecond range pulse duration respectively.

CHAPTER 3:

RESEARCH METHODOLOGY

3.1 Introduction

In this chapter, the fabrication and characterization of the proposed SA, which is obtained by embedding gold nanoparticles (GNPs) nanomaterials into a polyvinyl alcohol (PVA) film. By incorporating the SA in an EDFL, the laser generates stable Q-switching and mode-locking pulses. The configurations of both Q-switched and mode-locked lasers will also be described in this chapter.

3.2 Preparation of GNPs Based SA

Poly (sodium -4– styrenesulfonate) (PSSS) and gold (III) chloride trihydrate (~50% Au basis) ($HAuCl_4$) were purchased from Aldrich (Milwaukee, WI, USA), while tri–sodium citrate ($Na_3C_6H_5O_7$, TSC) and sodium borohydrate ($NaBH_4$) were purchased from R&M Marketing (U.K). Deionized water (resistivity 18.0 MΩ) was used for the preparation of all solutions. All chemicals and solvent were used as received without further purification. Reactions were carried out in the fume hood.

Au nanoparticles (NPs) used for this work were synthesized using a $NaBH_4$ reduction method. The Au NPs was prepared initially with an addition of 50 mL TSC, 3 mL PSSS and 3 mL of $NaBH_4$ into a beaker containing 1000 mL deionised water while stirring at 450 rpm. 50 mL $HAuCl_4$ (5 mL, in water) was added dropwise (~2 mL/min) into the mixture with continuous stirring followed by the addition of the excess amount of TSC (20 mL). The reaction was left for 5 minutes before continuing with centrifugation for cleaning purposes. The aqueous medium of Au NPs was undergoing colour change from yellowish to dark red or magenta during synthesis (Fig. 3.1(a)). The resulting magenta solution shows no further colour change. The resulting Au NPs was further used for fabrication as saturable absorber (SA) for pulses generation experiment.

The size was measured by using transmission electron microscopy (TEM) image together with the identification of NPs morphology. Fig. 3.1(c) and (d) shows the sizes and morphology of Au NPs observed from TEM and SEM image respectively. The spherical shape of plasmonic Au NPs have an average size of approximately ~5.46 nm. The NPs presented great stability and coexist in spherical morphology. They do not tend to agglomeration hence preventing in decreasing surface energy prior to stabilization cases.

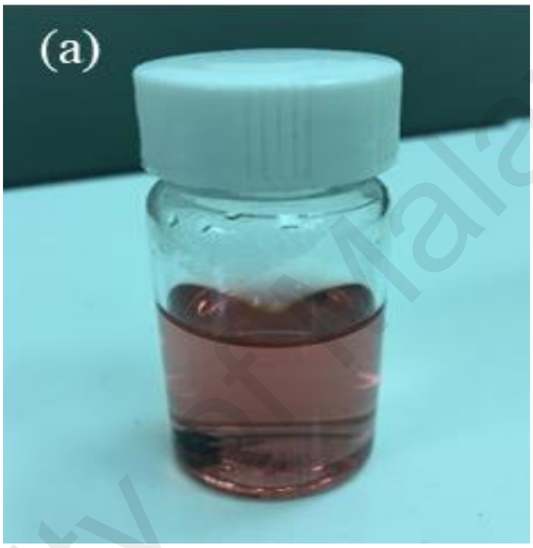

Figure 3.1(a): Gold nanoparticle (GNP) solution

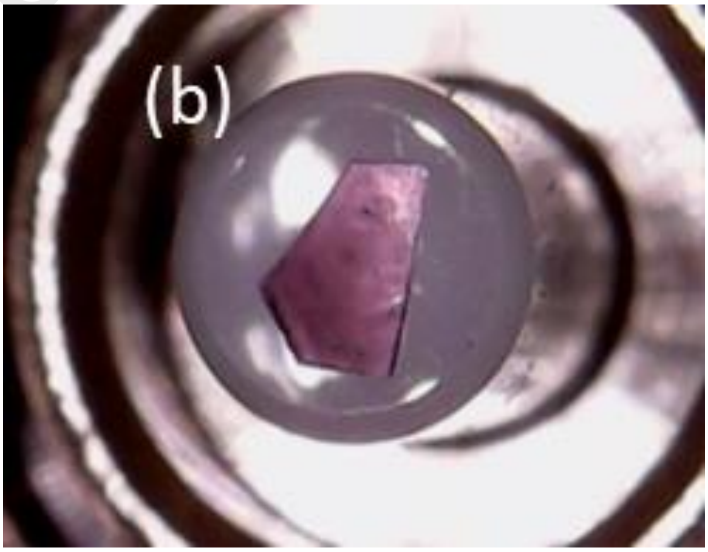

Figure 3.1(b): GNP PVA film

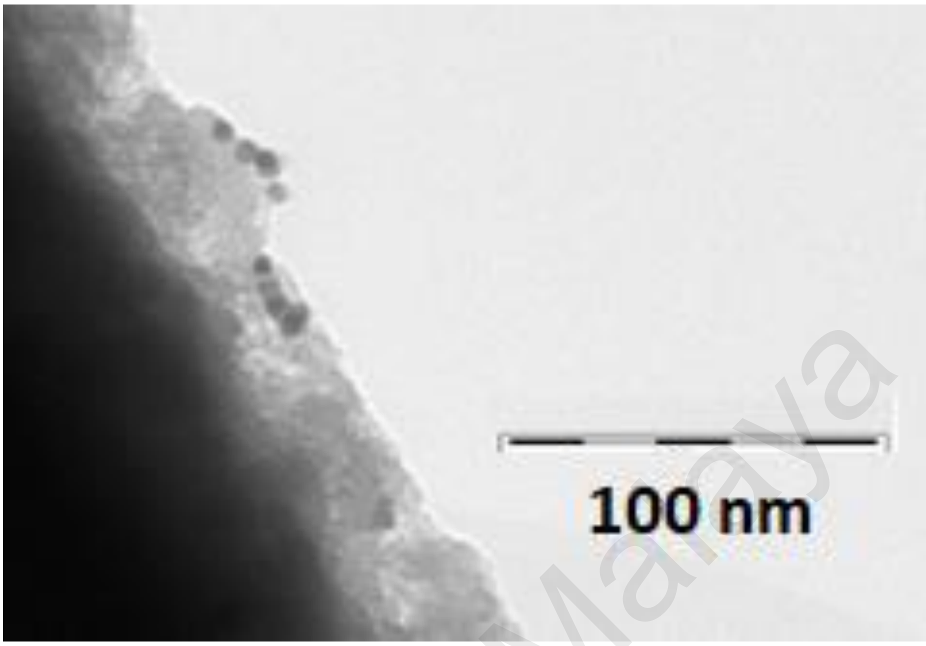

Figure 3.1(c): TEM image for AU NPs

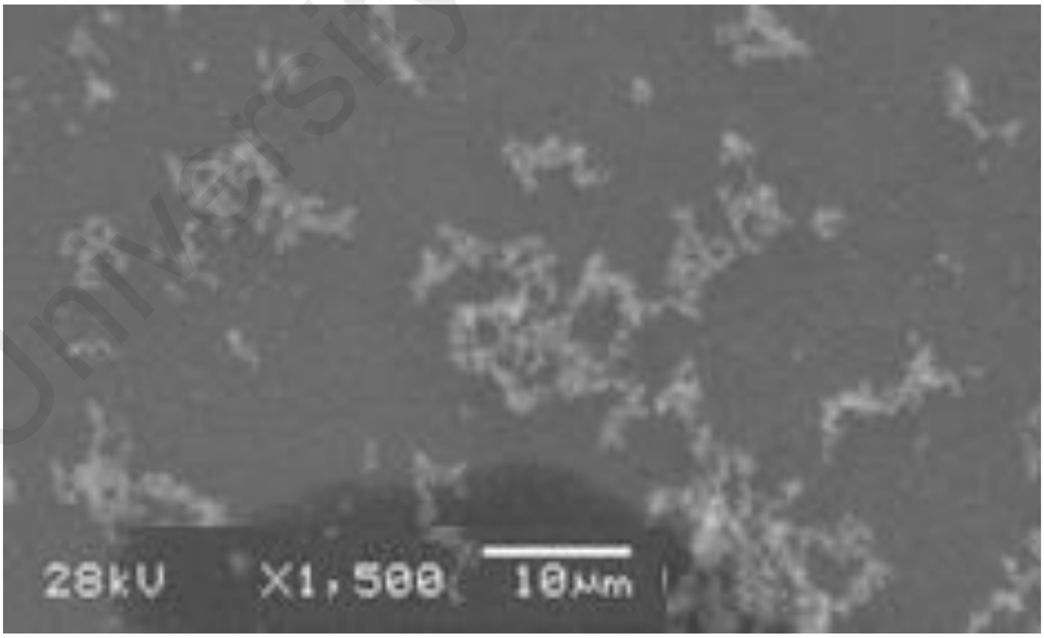

Figure 3.1(d): SEM image

The resulting gold nanoparticles solution was mixed with PVA solution to fabricate a SA film. The PVA solution was prepared by dissolving PVA powder (40000 MW, Sigma Aldrich) into 80 ml of DI water and then it is stirred at 145^{o} C until the powder completely dissolves. The mixture was slowly stirred for about 2 hours. The resulting suspension was then poured into the petri dish and left to dry at room temperature.

After 2 days, the thin film was slowly peeled from the petri dish. The gold nanoparticles PVA film was then cut into a small piece to be attached into an FC/PC fiber ferrule as shown in Fig. 3.1(b). The ferrule was then matched with another fresh ferrule via a fiber adaptor after depositing a small amount of index matching gel onto the fiber end to construct an all-fiber SA device.

The nonlinear optical properties of the gold nanoparticles PVA film was also investigated with a balanced twin-detector measurement technique. The illumination pulse is generated from a home-made mode-locked fiber laser (wavelength, 1.55 μm; pulse duration, ≈1.3 ps; repetition rate, ≈12.5 MHz). The nonlinear transmission of the film is measured by comparing the input power and output power with a double-channel powermeter.

As illustrated in Fig. 3.2, the fabricated film exhibits the saturable absorption property that the transmission (absorption) increases (decreases) with optical intensity. The modulation depth, saturable intensity and nonsaturable absorption of the film are obtained as 13.6 %, 0.5 MW/cm2 and 47.2%, respectively. It is worth noting that we have not observed any nonlinear response from pure PVA film, confirming that the saturable absorption property solely originates from the gold nanoparticles.

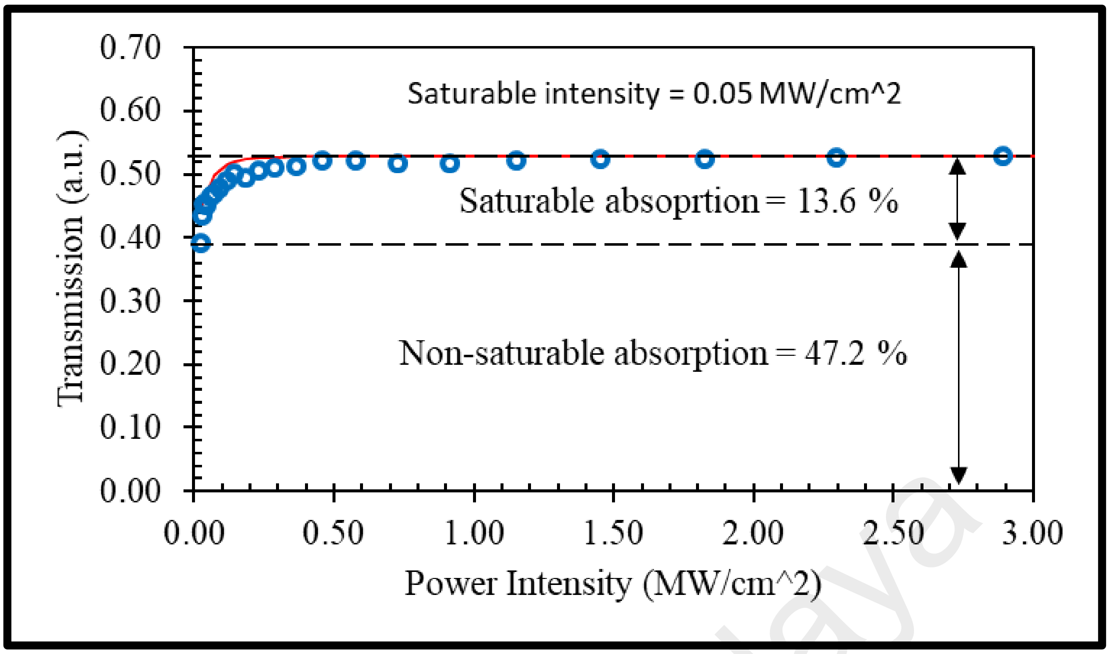

Figure 3.2: The non-linear optical properties of gold nanoparticle film by balance twin-detector measurement technique.

3.3 Experimental Setup

An EDFL was constructed to investigate the Q-switching performance of the newly developed GNP based SA film, as shown in Fig. 3.3. The fiber laser was composed of 2.8 m EDF with 90 dB/m absorption at 980 nm, a 980/1550 nm wavelength division multiplexer (WDM), an optical isolator, an SA device and a 90:10 output coupler. The EDF was pumped by a 980 nm laser diode via the WDM. The isolator was used to ensure unidirectional propagation of the oscilating laser in the ring laser cavity. A 90:10 optical coupler was used to extract 10% of the oscillating light from the cavity as a laser output.

The characteristics of the generated laser spectrum were monitored and analyzed using an optical spectrum analyzer with 0.02 nm resolution (Yokogawa AQ6370C). An oscilloscope (GWINSTEK: GDS-3352) with high speed photodetector were used to monitor the output pulse trains. The repetition rate and the stability of the Q-switched laser is measured using 7.8 GHz Radio Frequency (RF) spectrum analyzer (Anritsu MS2683A). An average output power was measured by the power meter (Thorlabs PM 100D) coupled with its power head (S145C Integrating sphere Photodiode Power Sensor, InGaAs, 800-1700 nm @3W) . The overall length of the laser cavity was approximately 14.8 m.

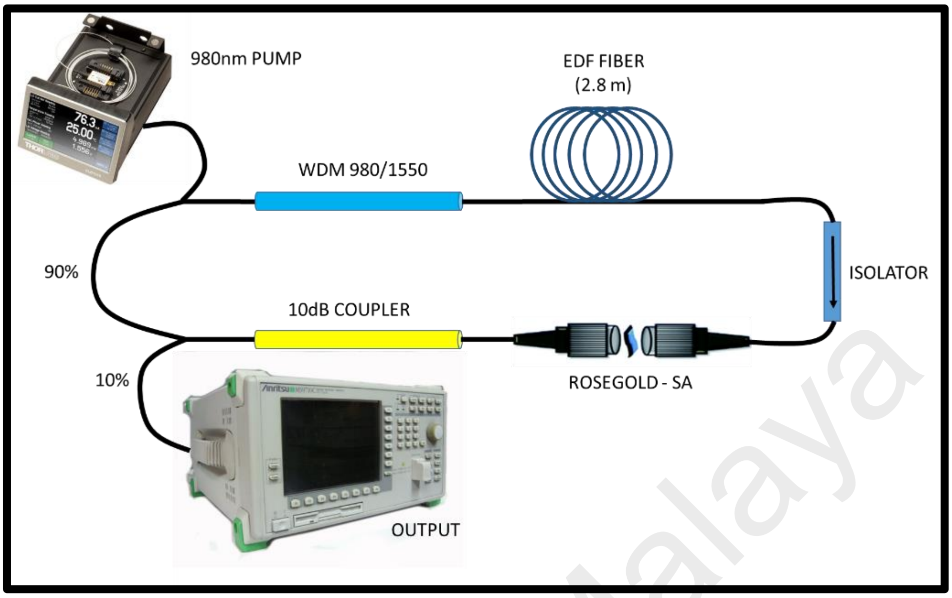

Figure 3.3: Schematic configuration of Q-switched fiber laser utilizing GNP PVA SA.

The laser cavity was modified to allow mode-locking operation by adding an additional single-mode fiber (SMF) length as shown in Fig. 3.4. The 200 m long SMF was added into the cavity to tailor the dispersion characteristic and nonlinearity of the cavity and allow mode-locking pulses generation. The total length of cavity becomes 214.8 m, which consists of 200 m standard SMF, 1m of WDM fiber and 2.8 m of EDF. The group velocity dispersion (GVD) of the SMF, WDM fiber and EDF are -21.9 ps^2/km, -38 ps^2/km and -21.6 ps^2/km, respectively. Therefore the group delay dispersion inside the cavity was calculated to be around -4.4 ps^2, which indicates the mode-locked laser operates in anamolous dispersion regime.

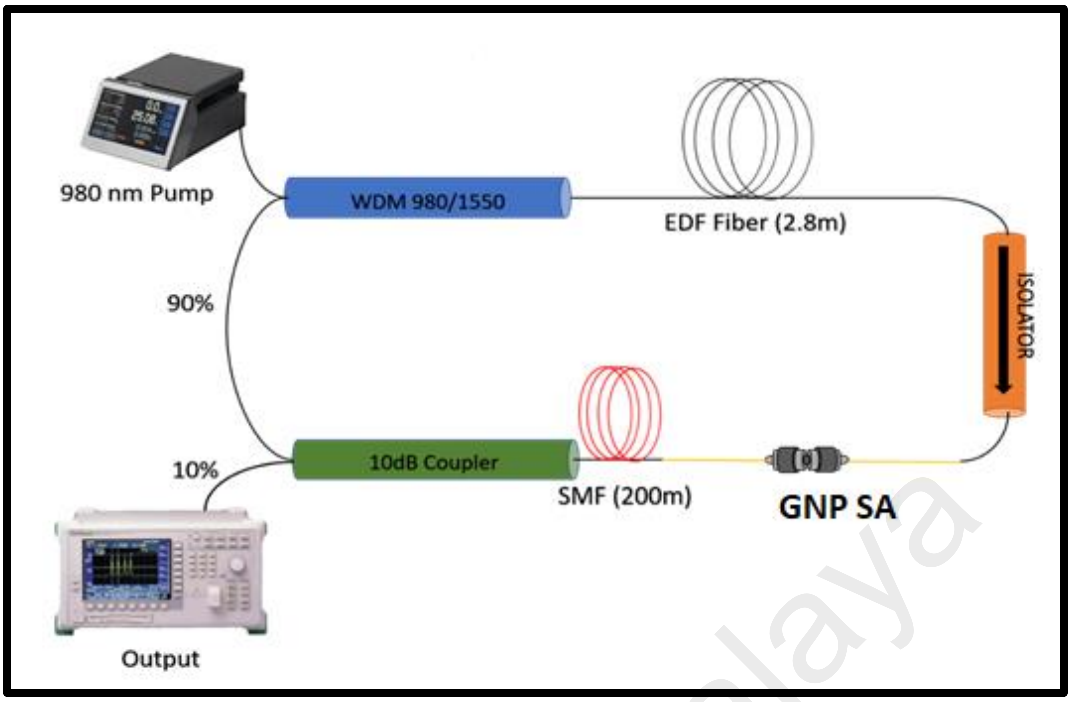

Figure 3.4: Schematic configuration of the mode-locked fiber laser utilizing GNP PVA SA.

CHAPTER 4:

RESULTS AND DISCUSSION

4.1 Introduction

Pulsed lasers are of great importance due to their wide range of applications such as medical surgery and material processing. Q-switched pulsed laser is normally used for micromachining and surgery which require high pulse energy while mode-locked lasers with narrow pulse width and high repetition rate are employed for high speed optical signal processing. Pulsed fiber lasers are more attractive than their counterparts due to their compactness, simplicity, alignment free operation and low cost. Compared to active method, pulse generation by passive method using saturable absorber (SA) is a more popular and viable method. SA has characteristics where light absorbance decreases with the increase of light intensity. In this chapter, Q-switched and mode-locked Erbium-doped fiber lasers (EDFLs) are demonstrated using a new thin film SA, which was developed based on GNPs based SA.

4.2 Q-Switching Operation

Q-switched fiber lasers are widely employed in applications which require high pulse energy such as range finding, remote sensing, optical communication, laser processing, and etc. (Grudinin, 2013; C. Xu & Wise, 2013). They are typically obtained based on the modulation of the quality factor, Q of a cavity, which can be realized by either active or passive technique. Compared with the active technique, passive Q-switching based on intensity saturable absorbers (SAs) possesses the advantages of compactness, low cost, and simple cavity configuration. It has been reported that various kinds of functional materials are used as SAs to achieve passive Q-switching, such as graphene (Bao-Quan et al., 2014), gold nanorods (Wang et al., 2014), carbon nanotubes (Zuikafly, Ahmad, Ibrahim, Latiff, & Harun, 2016), Bi_2Se_3 (Sobon, 2015), MoS_2 (Kadir, Ismail, & Latiff, 2017), WS_2 (Yan, Liu, et al., 2015), and so on. Besides, exploring other new SA materials and designing new schemes of passive Q-switching EDFLs is still attractive.

Despite many methods and new materials are explored in developing the SA for Q-switching pulse generation, metal nanoparticles-based SA especially transition metal elements are rarely being investigated. These elements pick up a great interest amongst scientific researchers as they hold a unique optical property such as ultrafast response time, broad saturable absorption band and large third-order nonlinearity (Sobon, 2015). Very recently, Duanduan Wu et. al. reported a Q-switch pulse generation by using Copper Nanowires (CuNW) as saturable absorber at visible range laser region (635 nm) with repetition rate ranging from 239.8 – 312.4 kHz, pulse width of 0.685 - 0.394 μs and maximum output power up to 9.6 mW (Wu et al., 2016). The visible 635 nm Q-switched fiber laser was also reported using Gold nanoparticle (GNP) in Praseodymium (Pr^{3+})-doped fiber laser cavity.

In this section, we propose and demonstrate a passively Q-switched fiber laser using GNP, which is embedded in polymer film as a SA. The laser generates Q-switching pulse train with pulse width of 4.16 μs, repetition rate of 56.8 kHz and output power of 0.18 mW at the maximum input power of 92.3 mW. Our results indicate that GNP has potential for pulse generation in the 1550 nm region.

In this experiment, 980 nm pump power was slowly increased until we obtained a stable Q-switched pulse train. Stable, robust and self-starting Q-switching oscillation was obtained as soon as the incident pump power exceeded the threshold of 63.4 mW. There is no lasing below the threshold pump power. Such a low threshold power for Q-switching operation resulted from the small intra-cavity loss performed by the GNPs PVA SA. The spectral and temporal characteristics of the Q-switched laser is presented in Figs. 4.1 and 4.2, respectively. **Fig. 4.1** shows the spectrum of the laser at a pump power of 63.4 mW, which centered at a wavelength of 1564.2 nm. It shows an obvious spectral broadening due to self-phase modulation effect in the ring cavity. **Fig. 4.2** illustrates the typical oscilloscope trace of the Q-switched fiber laser at a pump power of 63.4 mW. It shows the peak to peak duration of 20.2 μs, which can be translated to the repetition rate of 49.4 kHz. The Q-switching pulses output was stable and no amplitude modulation was observed in the pulses train. This shows that there was no self-mode locking (SML) effect during the Q-switching operation.

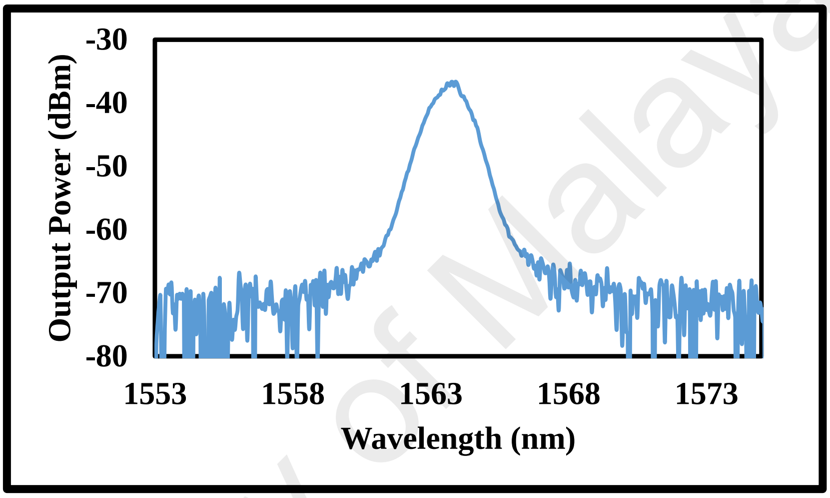

Figure 4.1: Output spectrum of the Q-switched EDFL at a pump power of 63.4 mW

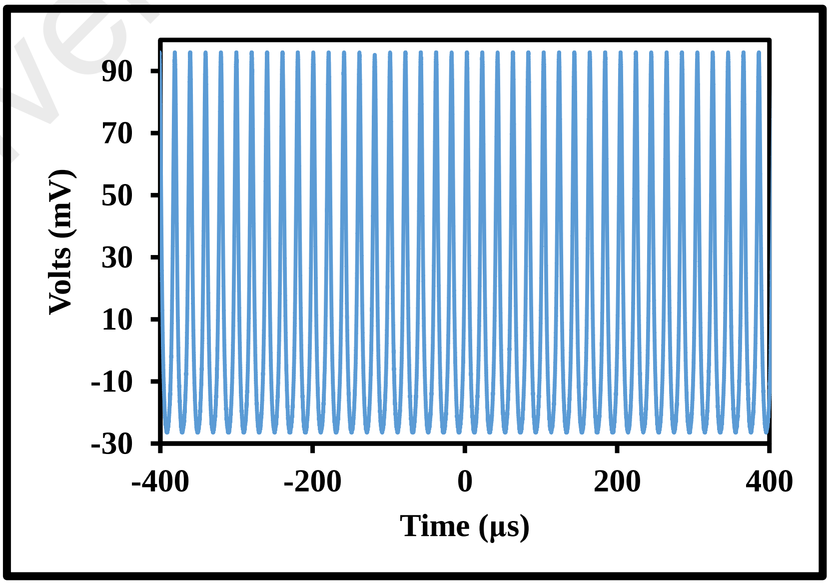

Figure 4.2: Typical oscilloscope trace of the Q-switched EDFL at a pump power of 63.4 mW

Fig. 4.3 shows the RF spectrum of the Q-switching pulses at a pump power of 63.4 mW. The spectrum indicates the fundamental frequency at 49.4 kHz with a signal to noise ratio (SNR) of more than 35 dB. The high SNR indicates an excellent pulse train stability, comparable to other Q-switched fiber lasers. To verify that the passive Q-switching was attributed to the GNPs film, the SA device was removed from the ring cavity. In this case, no Q-switched pulses were observed on the oscilloscope even when the pump power was adjusted over a wide range. This finding confirmed that the GNPs PVA SA was responsible for the passively Q-switched operation of the laser. GNPs possess saturable absorption band in the 1550 nm region induced by surface plasmon resonance (SPR).

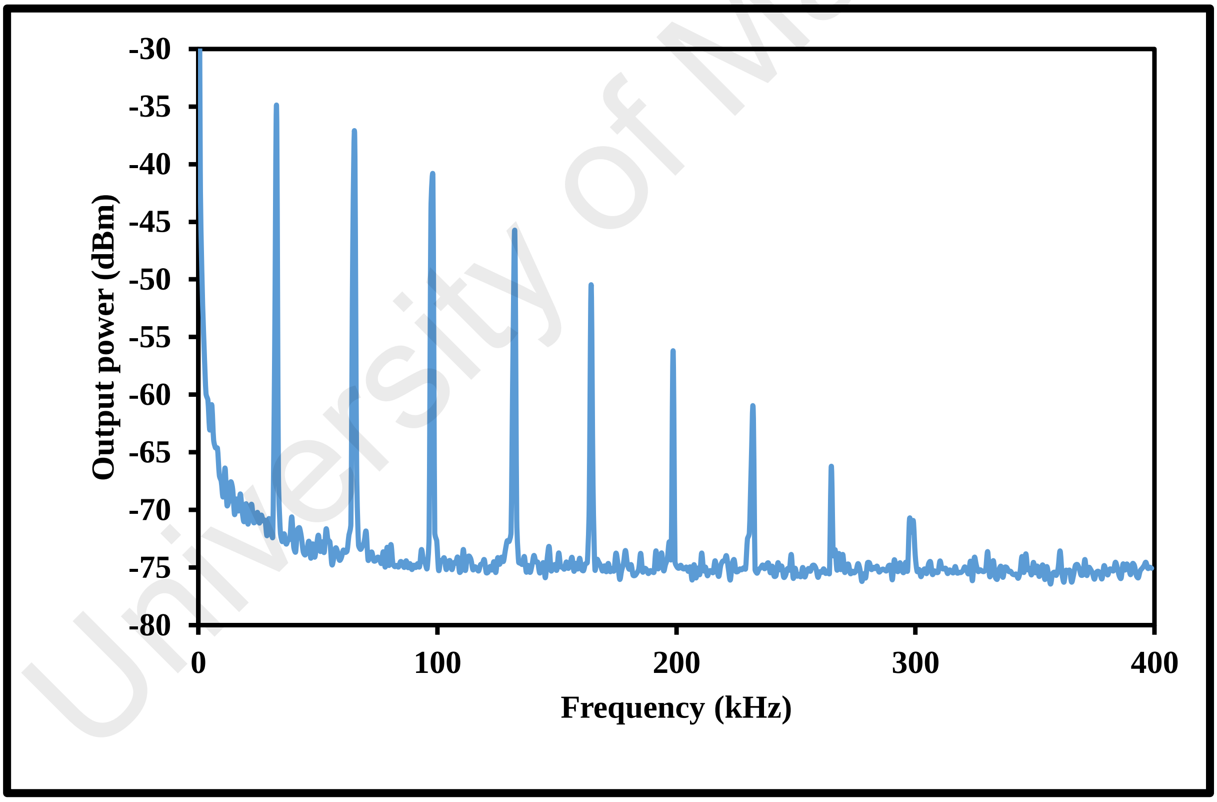

Figure 4.3: RF spectrum of the Q-switched EDFL at a pump power of 63.4 mW

Fig. 4.4 draws the variation tendency curves of pulse repetition rate and pulse width with the incident pump power. When the pump power is varied from 63.4 mW to 92.3 mW, the repetition rate increases almost linearly from 49.4 to 56.8 kHz. This is a typical characteristic of the Q-switched laser, which is mainly due to the higher pump power provides more gain to saturate the SA. On the other hand, pulse duration reduces from 5.56 µs to 4.16 µs as the pump power increases within the same range.

We observe a smaller reduction of pulse width as the pump power increases. This is due to the fact that the SA is becoming saturated when more photons circulate inside the laser cavity as the pump power increased. The minimum attainable pulse duration is 4.16 µs, which is believed to be related to the modulation depth of the SA. The pulse duration can be further decreased by shortening the cavity length and improving the modulation depth of the SA.

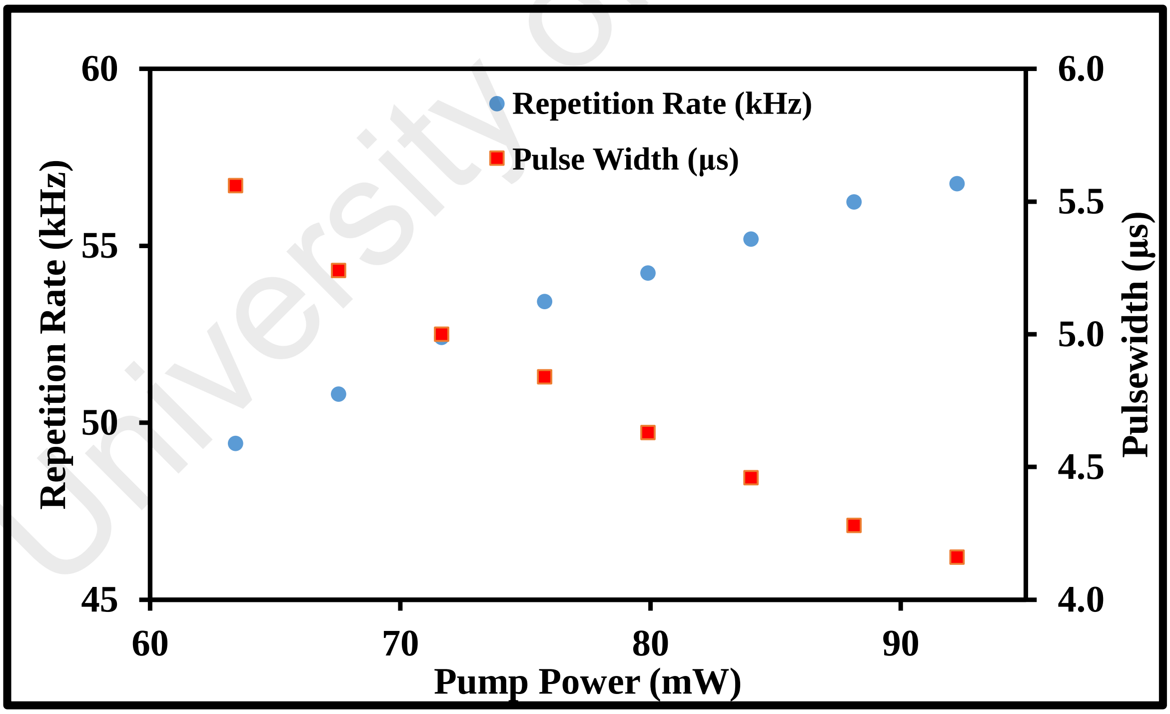

Figure 4.4: Repetition rate and pulse width against the pump power

Fig. 4.5 shows the output power and pulse energy as a function of the incident pump power. The output power increases linearly at first and then becomes saturated. Likewise, the pulse energy increases linearly before it saturates and even slightly decreases at higher pump power. These are most probably due to the bleaching and thermal accumulation effects of the GNPs SA under high pump intensity. It is observed that the output power can recover again as we decreased the incident pump power, indicating no damage of the GNPs SA. At the pump power of 92.8 mW, the maximum output power was measured to be 0.18 mW. The maximum pulse energy of 3.1 nJ was obtained with the pump power of 92.3 mW. It is expected that the higher pulse energy could be achieved by further improving the quality of GNPs SA, or optimizing the cavity designs.

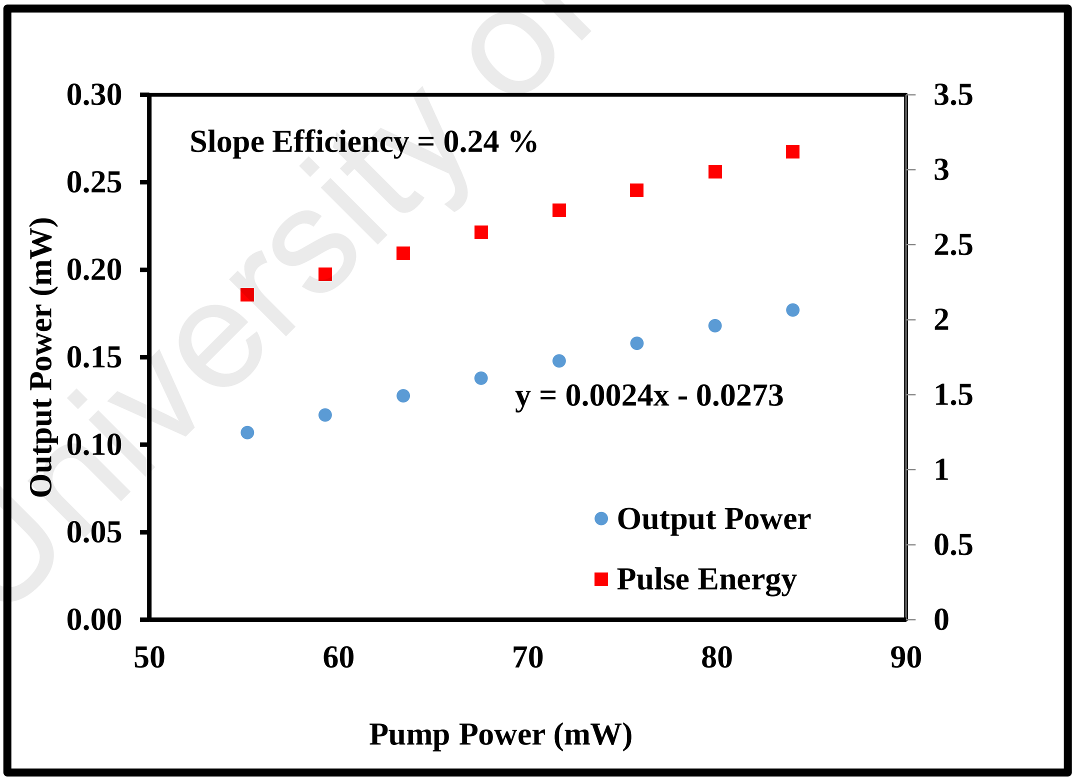

Figure 4.5: Output power and pulse energy against the pump power

4.3 Mode-Locking Operation

Nanosecond pulses are attractive for potential use in generating high pulse energy laser sources for many industrial and scientific applications, such as micromachining, metrology, bio-medicine, and telecommunications (Clowes, 2008; Dornfeld, Min, & Takeuchi, 2006; Luo, Chu, & Liu, 2000). Nanosecond pulse fiber lasers have normally low repetition rates of around few MHz, which is convenient for reaching microjoule energies through external amplification. Conventionally, nanosecond pulses lasers were achieved by active modulation approach utilizing electro-optic and acousto-optic modulators, which is bulky and high cost. The nanosecond laser can also be realized by passive technique based on Q-switching and mode-locking. Passively Q-switched lasers mainly use crystal based saturable absorber, such as Cr:YAG, as a Q-switcher.

However, a stable pulse train is difficult to achive by this approach. On the other hand, stable nanosecond pulses can be obtained by extension of the cavity length in a passively mode-locked fiber laser using nonlinear polarization rotation (NPR) technique (Mao, Liu, Wang, Hu, & Lu, 2010; Mao, Liu, Wang, Lu, & Feng, 2010) or semiconductor saturable absorber mirror (SESAM) (L. Chen et al., 2009). However, NPR based mode-locked fiber laser is relatively low environmental stability and reliability since it requires the adjustment of the polarization state of the oscillating light in the cavity. SESAMs have recently become readily available, but it is still quite expensive for purposes of large scale of production.

Recently, two-dimensional (2D) nanomaterials such as graphene, black phosphorus, transition metal dichalcoganides (TMDs), topological insulators (TI) have attracted a great deal of interest for application in saturable absorber (SA) (Bao et al., 2009; Hisyam, Rusdi, Latiff, & Harun, 2016; Yan, Lin, et al., 2015). Most of these works were focused on obtaining Q-switching pulses with microsecond pulse width and mode-locking pulses with femtosecond or picosecond pulse width. Only a few works have been reported on generating nanosecond pulse. For instance, Xu et al demonstrated a mode-locked nanosecond EDFL using a graphene SA (J. Xu et al., 2012).

On the other hand, many researchers explored on metals nanoparticles as SAs in more recent years for constructing Q-switched and mode-locked fiber lasers due to the broadband absorption induced by the surface plasmon resonance and fast time response with a scale of picosecond. This has been demonstrated by (Jiang et al., 2012; Kang, Guo, et al., 2013; Kang, Xu, et al., 2013) using Yb, Er and Tm fiber laser based on gold by controlling the Sp peak at 1030 nm, 1550 nm and 1950 nm in order to investigate the potential of metal nanomaterials. The gold shows a great third order nonlinearity, which makes it a suitable SA for generating mode-locking and Q-switching pulses. Moreover, the gold nanoparticle is a noble metal, which has close lying band that allows the electron to move freely. The energy has occupied the electron on the conduction band before it is excited to surface plasmon resonance band when light beam hits the gold particles (Gurudas et al., 2008).

In this section, we report the gold nanoparticles is used to generate stable nanosecond pulses from an EDFL in a long ring cavity. The surface plasmon resonance (SPR) of gold nanoparticles enables the generation of mode-locked laser operating at 1567.0 nm with constant repetition rate of 970 kHz and the maximum pulse energy of 25.5 nJ at the pump power of 187 mW.

In this experiment, the continuous wave (CW) laser operation started at an input pump power of about 84 mW and the self-started mode-locking occurred at about 145.8 mW. The relatively high threshold of CW operation could be attributed to large inserting loss and long cavity. The mode-locked operation was maintained and was stable until the pump power reached 187 mW and operated the the fundamental frequency of 970 kHz. The mode-locked laser optical spectrum at the threshold pump power of 145.8 mW is shown in **Fig. 4.6**, which operated at the centre wavelength of 1567.0 nm with 3dB spectral bandwidth of 1.1 nm.

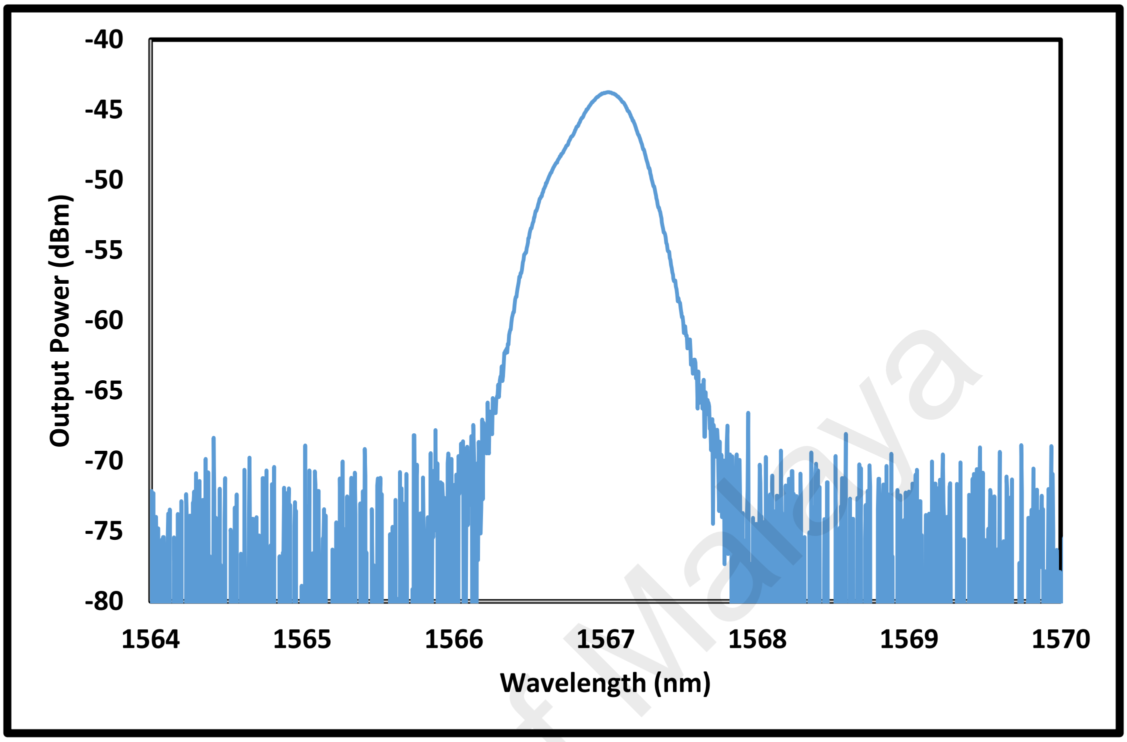

Figure 4.6: Output spectrum of the mode-locked EDFL at a pump power of 145.8 mW

Fig. 4.7 shows the oscilloscope trace of the mode-locked pulse train. The time interval between the pulses is about 1 µs, that matches with cavity length of 214.8 m. The repetition rate of the soliton pulses is kept to be 970 kHz, when adjusting the value of pump power from 145.8 to 187.0 mW. This operation mode is very stable with respect to any environmental perturbations and fluctuations of the pump power. **Fig. 4.8** shows an enlarged figure of the oscillocope trace, which indicates the pulse width of 450 ns. We found that no bunched pulses were observed in the pulse internal structure, thus the observed nanosecond pulse was a clean and stable single pulse. The mode-locked operated in cavity consist of anamolous dispersion with group velocity dispersion about -4.25 ps2.

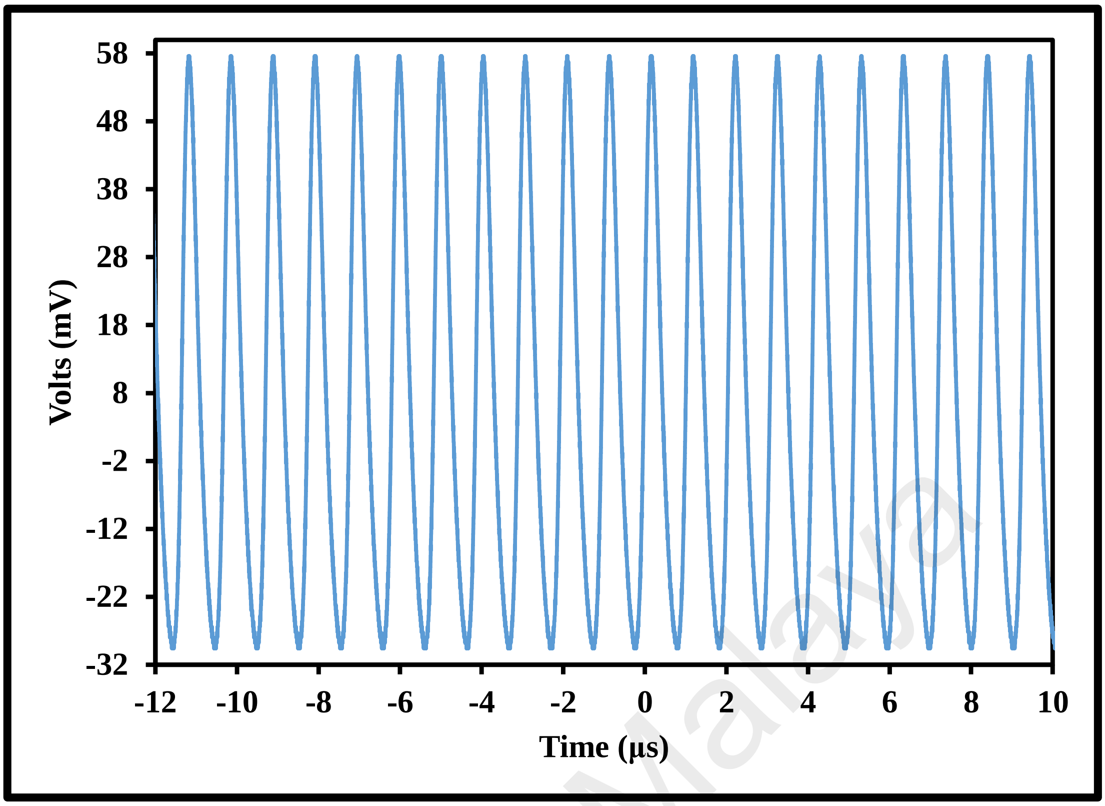

Figure 4.7: Typical oscilloscope trace of the mode-locked EDFL at a pump power of 145.8 mW

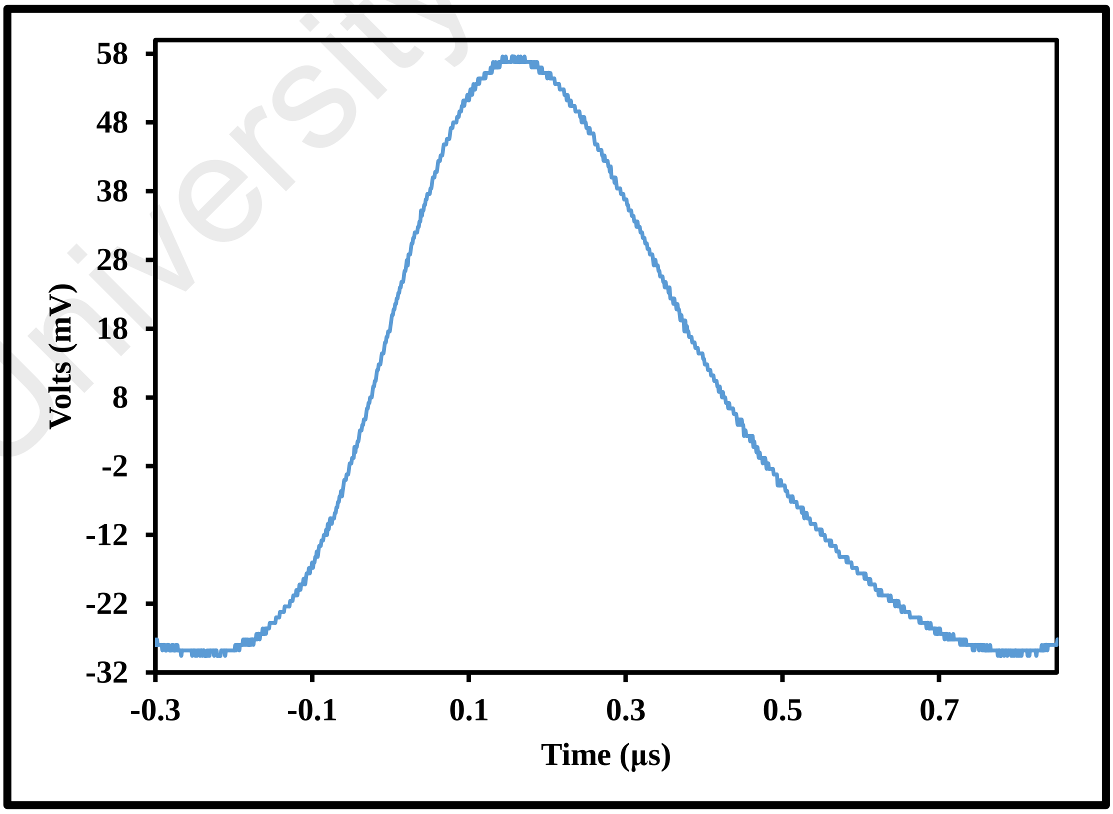

Figure 4.8: Single envelop of the oscilloscope trace

The stable nanosecond output pulses was confirmed with the radio frequency spectrum as indicated in **Figure 4.9**. It provides signal to noise ratio (SNR) as high as 51 dB for the fundamental frequency. The peak of the fundamental frequency decreases moderately until 4th harmonic, which indicates a pulse width in nanosecond regime. There are no presence of mode-locked pulses when the SA was removed. The relationship between the output average power and pulse energy with respect to incident pump power is shown in **Figure 4.10**. It can be seen that the output power increases monotonously with the pump power with a slope efficiency of 1.4 %. The efficiency is quite low due to the use of a ultra short gain medium length and long cavity length. The average output power increases from 1.91 mW to 2.48 mW as the pump power rises from 145.8 mW to 187.0 mW. The single pulse energy also increases linearly with the pump power. The maximum pulse energy of 25.5 nJ was obtained at pump power of 187.0 mW. The experimental results verify the mode-locking ability of the newly developed gold nanoparticles based SA. This shows that the gold nanoparticles could be used in optoelectronics device and communication device in the C band region.

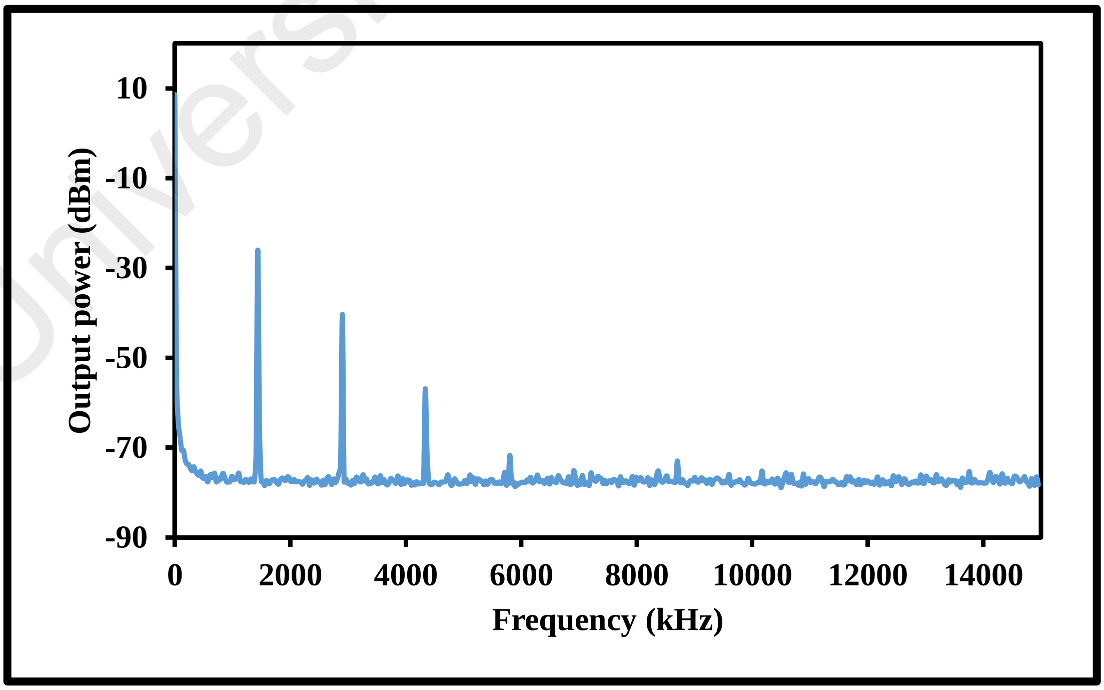

Figure 4.9: Typical RF spectrum of the mode-locked EDFL at a pump power of 145.8 mW

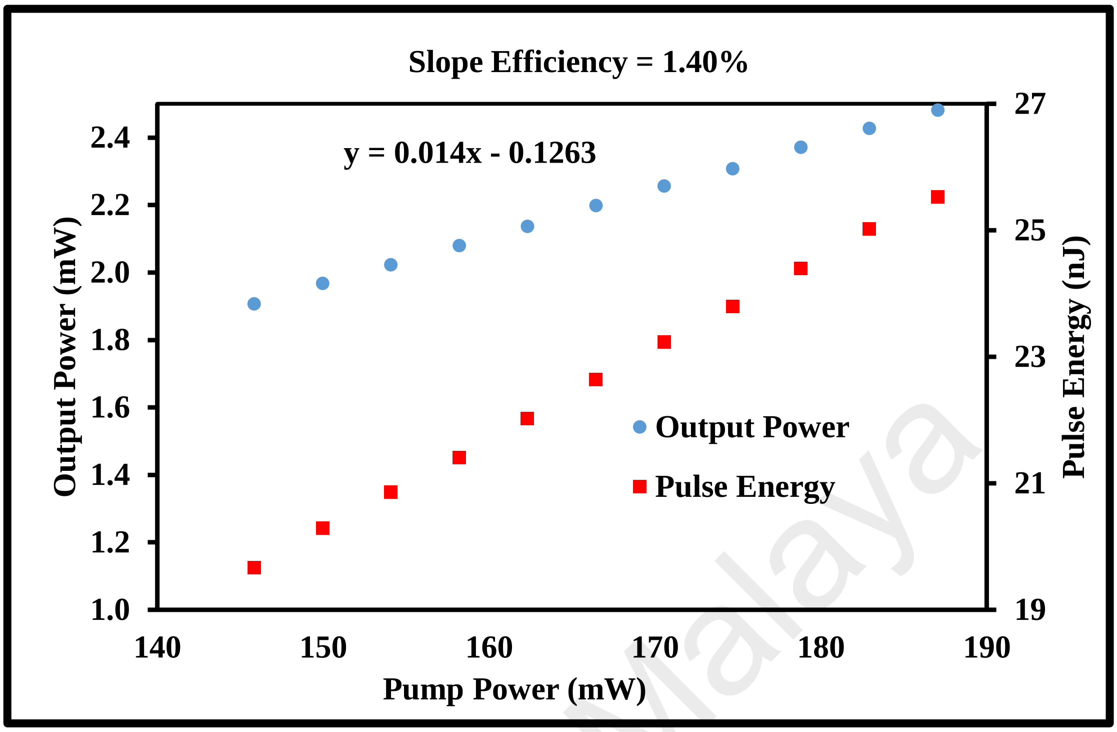

Figure 4.10: The relationship between pump power with output power and pulse energy.

CHAPTER 5:

CONCLUSION

We have successfully demonstrated Q-switched and mode-locked Erbium-doped fiber lasers (EDFLs) using gold nanoparticles (GNPs), which is embedded into a PVA film as a passive SA. The gold nanoparticles were prepared by a simple NaBH4 reduction method and embedded into PVA film to fabricate SA device. The fabricated film shows a modulation depth of 13.6 % and a saturable optical intensity of 0.5 MW/cm^2. The film was sandwiched between two ferrules via a fiber connector to form a fiber-compatible SA. Stable Q-switched pulses train operating at 1564.2 nm was successfully achieved within the incident pump power range from 63.4 mW to 92.3 mW. The repetition rate ranges from 49.4 to 56.8 kHz and the pulse width can be as narrow as 4.16 μs. The highest pulse energy of 3.1 nJ was obtained at 92.3 mW pump power. Stable mode-locked nanosecond pulses at 1567 nm with spectral width of 1.1 nm, pulse duration of 450 ns and a fundamental repetition rate of 970 kHz have been obtained. The average output power was 2.48 mW, corresponding to single pulse energy of 25.5 nJ at pump power of 187 mW. These results exhibit that the GNPs PVA film has good saturable absorption ability in the 1550 nm spectral region. The experimental results suggest that multilayer gold nanoparticles is a promising material for ultrafast laser applications.

REFERENCES

Addanki, S., Amiri, I., & Yupapin, P. (2018). Review of optical fibers-introduction and applications in fiber lasers. *Results in Physics, 10*, 743-750.

Agrawal, G. (2001). *Applications of nonlinear fiber optics*: Elsevier.

Ahmed, M. H. M. (2015). *Development of Q-Switched and Mode-locked Erbium Doped Fiber Lasers Based on Carbon Nanotubes Saturable Absorbers.* Jabatan Kejuruteraan Elektrik, Fakulti Kejuruteraan, Universiti Malaya.

Ainslie, B. J., Craig, S. P., & Davey, S. T. (1988). The absorption and fluorescence spectra of rare earth ions in silica-based monomode fiber. *Journal of lightwave technology, 6*(2), 287-293.

Astakhov, A., Butusov, M., Galkin, S., Ermakova, N., & Fedorov, Y. K. (1987). Fiber laser with 1.54-µm radiation wavelength. *Optics and Spectroscopy, 62*, 140-141.

Bao-Quan, Y., Zheng, C., Xiao-Ming, D., Ying-Jie, S., Ji, W., & Yan-Qiu, D. (2014). A graphene-based passively Q-switched Ho: YAG laser. *Chinese Physics Letters, 31*(7), 074204.

Bao, Q., Zhang, H., Wang, Y., Ni, Z., Yan, Y., Shen, Z. X., . . . Tang, D. Y. (2009). Atomic-layer graphene as a saturable absorber for ultrafast pulsed lasers. *Advanced Functional Materials, 19*(19), 3077-3083.

Carruthers, T. F., Duling, I., & Dennis, M. L. (1994). Active-passive modelocking in a single-polarisation erbium fibre laser. *Electronics Letters, 30*(13), 1051-1053.

Chen, H.-R., Tsai, C.-Y., Cheng, H.-M., Lin, K.-H., & Hsieh, W.-F. (2014). Passive mode locking of ytterbium-and erbium-doped all-fiber lasers using graphene oxide saturable absorbers. *Optics express, 22*(11), 12880-12889.

Chen, L., Zhang, M., Zhou, C., Cai, Y., Ren, L., & Zhang, Z. J. E. l. (2009). Ultra-low repetition rate linear-cavity erbium-doped fibre laser modelocked with semiconductor saturable absorber mirror. *45*(14), 731-733.

Chernysheva, M., Mou, C., Arif, R., AlAraimi, M., Rümmeli, M., Turitsyn, S., & Rozhin, A. (2016). High power Q-switched thulium doped fibre laser using carbon nanotube polymer composite saturable absorber. *Scientific reports, 6*, 24220.

Clowes, J. (2008). Next generation light sources for biomedical applications. *Optik & Photonik, 3*(1), 36-38.

Csele, M. (2011). *Fundamentals of light sources and lasers*: John Wiley & Sons.

Degnan, J. J. (1989). Theory of the optimally coupled Q-switched laser. *IEEE Journal of Quantum Electronics, 25*(2), 214-220.

DeMaria, A., Stetser, D., & Heynau, H. (1966). Self mode-locking of lasers with saturable absorbers. *Applied Physics Letters, 8*(7), 174-176.

Desurvire, E., & Simpson, J. R. (1989). Amplification of spontaneous emission in erbium-doped single-mode fibers. *Journal of lightwave technology, 7*(5), 835-845.

Digonnet, M. J. (2001). Rare-earth-doped fiber lasers and amplifiers.

Dong, L., & Samson, B. (2016). *Fiber Lasers: Basics, Technology, and Applications*: CRC Press.

Dornfeld, D., Min, S., & Takeuchi, Y. (2006). Recent advances in mechanical micromachining. *CIRP Annals-Manufacturing Technology, 55*(2), 745-768.

Fermann, M. E., & Hartl, I. (2013). Ultrafast fibre lasers. *Nature photonics, 7*(11), 868.

France, P. (1988). *Optical Loss Mechanisms in Fluorozirconate Glasses and Infrared Fibres.* University of Sheffield, Department of Ceramics, Glasses and Polymers.

Grudinin, A. (2013). Fibre laser directions. *Nature Photonics, 7*(11), 846-847.

Gursel, A. T. (2018). Fiber Lasers and Their Medical Applications *Optical Amplifiers-A Few Different Dimensions*: IntechOpen.

Gurudas, U., Brooks, E., Bubb, D. M., Heiroth, S., Lippert, T., & Wokaun, A. (2008). Saturable and reverse saturable absorption in silver nanodots at 532 nm using picosecond laser pulses. *Journal of Applied Physics, 104*(7), 073107.

Haus, H. A. (2000). Mode-locking of lasers. *IEEE Journal of Selected Topics in Quantum Electronics, 6*(6), 1173-1185.

Hisyam, M., Rusdi, M., Latiff, A., & Harun, S. (2016). Generation of Mode-locked Ytterbium doped fiber ring laser using few-layer black phosphorus as a saturable absorber. *IEEE Journal of selected topics in quantum electronics*.

Hudson, D. D. (2009). *Mode-locked fiber lasers: Development and application.* Citeseer.

Jabczyński, J. K., Zendzian, W., & Kwiatkowski, J. (2006). Q-switched mode-locking with acousto-optic modulator in a diode pumped Nd: YVO 4 laser. *Optics express, 14*(6), 2184-2190.

Jiang, T., Xu, Y., Tian, Q., Liu, L., Kang, Z., Yang, R., . . . Qin, W. (2012). Passively Q-switching induced by gold nanocrystals. *Applied Physics Letters, 101*(15), 151122.

Kadir, N., Ismail, E., & Latiff, A. (2017). Transition Metal Dichalcogenides (WS2 and MoS2) Saturable Absorbers for Mode-Locked Erbium-Doped Fiber Lasers. *Chinese Physics Letters, 34*(01), 14202.

Kang, Z., Guo, X., Jia, Z., Xu, Y., Liu, L., Zhao, D., . . . Qin, W. (2013). Gold nanorods as saturable absorbers for all-fiber passively Q-switched erbium-doped fiber laser. *Optical materials express, 3*(11), 1986-1991.

Kang, Z., Xu, Y., Zhang, L., Jia, Z., Liu, L., Zhao, D., . . . Qin, W. (2013). Passively mode-locking induced by gold nanorods in erbium-doped fiber lasers. *Applied Physics Letters, 103*(4), 041105.

Keller, U., & Paschotta, R. (2002). Ultrafast solid-state lasers *Ultrafast Lasers* (pp. 17-65): CRC Press.

Keller, U., Weingarten, K. J., Kartner, F. X., Kopf, D., Braun, B., Jung, I. D., . . . Der Au, J. A. (1996). Semiconductor saturable absorber mirrors (SESAM's) for femtosecond to nanosecond pulse generation in solid-state lasers. *IEEE Journal of Selected Topics in Quantum Electronics, 2*(3), 435-453.

Koester, C. (1966). 9A4-Laser action by enhanced total internal reflection. *IEEE Journal of Quantum Electronics, 2*(9), 580-584.

Koester, C. J., & Snitzer, E. (1964). Amplification in a fiber laser. *Applied optics, 3*(10), 1182-1186.

Lee, Y.-W., Chen, C.-M., Huang, C.-W., Chen, S.-K., & Jiang, J.-R. (2016). Passively Q-switched Er 3+-doped fiber lasers using colloidal PbS quantum dot saturable absorber. *Optics express, 24*(10), 10675-10681.

Li, F., Zhu, H., & Zhang, Y. (2015). High-power widely tunable Q-switched thulium fiber lasers. *Laser Physics Letters, 12*(9), 095102.

Lü, X., Han, Q., Liu, T., Chen, Y., & Ren, K. (2014). Actively Q-switched erbium-doped fiber ring laser with a nanosecond ceramic optical switch. *Laser Physics, 24*(11), 115102.

Luo, L., Chu, P., & Liu, H. (2000). 1-GHz optical communication system using chaos in erbium-doped fiber lasers. *IEEE Photonics Technology Letters, 12*(3), 269-271.

Malmström, M., Margulis, W., Tarasenko, O., Pasiskevicius, V., & Laurell, F. (2012). Soliton generation from an actively mode-locked fiber laser incorporating an electro-optic fiber modulator. *Optics express, 20*(3), 2905-2910.

Mao, D., Liu, X., Wang, L., Hu, X., & Lu, H. J. L. P. L. (2010). Partially polarized wave-breaking-free dissipative soliton with super-broad spectrum in a mode-locked fiber laser. *8*(2), 134.

Mao, D., Liu, X., Wang, L., Lu, H., & Feng, H. J. O. e. (2010). Generation and amplification of high-energy nanosecond pulses in a compact all-fiber laser. *18*(22), 23024-23029.

Mears, R., Reekie, L., Poole, S., & Payne, D. (1986). Low-threshold tunable CW and Q-switched fibre laser operating at 1.55 μm. *Electronics Letters, 22*(3), 159-160.

Melton, C. N., Riahinasab, S. T., Keshavarz, A., Stokes, B. J., & Hirst, L. S. (2018). Phase transition-driven nanoparticle assembly in liquid crystal droplets. *Nanomaterials, 8*(3), 146.

Mocker, H. W., & Collins, R. (1965). Mode competition and self-locking effects in aq-switched ruby laser. *Applied Physics Letters, 7*(10), 270-273.

Mur, J. (2011). *Fiber Lasers*.

Poole, S., Payne, D. N., & Fermann, M. E. (1985). Fabrication of low-loss optical fibres containing rare-earth ions. *Electronics Letters, 21*(17), 737-738.

Popa, D., Sun, Z., Hasan, T., Torrisi, F., Wang, F., & Ferrari, A. (2011). Graphene Q-switched, tunable fiber laser. *Applied Physics Letters, 98*(7), 073106.

Shen, J. (2012). A compact diode-pumped Q-switched and mode-locked Nd: GdVO 4 laser based on SESAM. *Laser Physics, 22*(11), 1664-1666.

Shi, W., Schulzgen, A., Amezcua, R., Zhu, X., & Alam, S.-U. (2017). Fiber lasers and their applications: introduction. *JOSA B, 34*(3), FLA1-FLA1.

Snitzer, E. (1964). *Neodymium glass laser.* Paper presented at the Quantum Electronics.

Sobon, G. (2015). Mode-locking of fiber lasers using novel two-dimensional nanomaterials: graphene and topological insulators [Invited]. *Photonics Research, 3*(2), A56-A63. doi: 10.1364/PRJ.3.000A56

Sobon, G., Sotor, J., & Abramski, K. M. (2012). Passive harmonic mode-locking in Er-doped fiber laser based on graphene saturable absorber with repetition rates scalable to 2.22 GHz. *Applied Physics Letters, 100*(16), 161109.

Steinkemper, H., Fischer, S., Hermle, M., & Goldschmidt, J. (2013). Stark level analysis of the spectral line shape of electronic transitions in rare earth ions embedded in host crystals. *New Journal of Physics, 15*(5), 053033.

Sun, Z., Rozhin, A., Wang, F., Hasan, T., Popa, D., O'neill, W., & Ferrari, A. (2009). A compact, high power, ultrafast laser mode-locked by carbon nanotubes. *Applied Physics Letters, 95*(25), 253102.

Tippett, J. T., Borkowitz, D. A., Clapp, L. C., Koester, C. J., & Vanderburgh Jr, A. (1965). Optical and electro-optical information processing: MASSACHUSETTS INST OF TECH CAMBRIDGE.

Tiu, Z. C. (2015). *Development of bright and dark pulsed fiber laser based on nonlinear polarization rotation/Tiu Zian Cheak.* University of Malaya.

Urquhart, P. (1988). Review of rare earth doped fibre lasers and amplifiers. *IEE Proceedings J (Optoelectronics), 135*(6), 385-407.

Valdmanis, J., & Fork, R. (1986). Design considerations for a femtosecond pulse laser balancing self phase modulation, group velocity dispersion, saturable absorption, and saturable gain. *IEEE Journal of Quantum Electronics, 22*(1), 112-118.

Villegas, I., Cuadrado-Laborde, C., Abreu-Afonso, J., Díez, A., Cruz, J., Martínez-Gámez, M., & Andrés, M. (2011). Mode-locked Yb-doped all-fiber laser based on in-fiber acoustooptic modulation. *Laser Physics Letters, 8*(3), 227.

Wang, X.-D., Luo, Z.-C., Liu, H., Liu, M., Luo, A.-P., & Xu, W.-C. (2014). Microfiber-based gold nanorods as saturable absorber for femtosecond pulse generation in a fiber laser. *Applied Physics Letters, 105*(16), 161107.

Wu, D., Lin, H., Cai, Z., Peng, J., Cheng, Y., Weng, J., & Xu, H. (2016). Saturable Absorption of Copper Nanowires in Visible Regions for Short-Pulse Generation. *IEEE Photonics Journal, 8*(4), 1-7.

Xu, C., & Wise, F. W. (2013). Recent advances in fibre lasers for nonlinear microscopy. *Nat Photon, 7*(11), 875-882. doi: 10.1038/nphoton.2013.284

Xu, J., Wu, S., Liu, J., Wang, Q., Yang, Q.-H., & Wang, P. J. O. C. (2012). Nanosecond-pulsed erbium-doped fiber lasers with graphene saturable absorber. *285*(21-22), 4466-4469.

Yan, P., Lin, R., Ruan, S., Liu, A., Chen, H., Zheng, Y., . . . Hu, J. J. S. r. (2015). A practical topological insulator saturable absorber for mode-locked fiber laser. *5*, 8690.

Yan, P., Liu, A., Chen, Y., Wang, J., Ruan, S., Chen, H., & Ding, J. (2015). Passively mode-locked fiber laser by a cell-type WS2 nanosheets saturable absorber. *Scientific reports, 5*.

Yao, C., Thévenaz, L., & Brès, C. S. (2017). *Erbium doped random fiber laser and fiber mixing effect.* Paper presented at the Transparent Optical Networks (ICTON), 2017 19th International Conference on.

Zervas, M. N., & Codemard, C. A. (2014). High power fiber lasers: a review. *IEEE Journal of Selected Topics in Quantum Electronics, 20*(5), 219-241.

Zuikafly, S. N. F., Ahmad, F., Ibrahim, M. H., Latiff, A. A., & Harun, S. W. (2016). Dual-wavelength passively Q-switched Erbium-doped fiber laser with MWCNTs slurry as saturable absorber. *Photonics Letters of Poland, 8*(4), 98-100.